

Sym m etric M ass M atrix w ith Two Zeros
 in S U S Y S O (10) G U T , Lepton F lavor V iolations
 and Leptogenesis

M asako Bando ^{a; 1}, Satoru K aneko ^{b; 2}, M idori Obara ^{c; 3}
 and
 M orim itu Tanimoto ^{d; 4}

^a Aichi University, Aichi 470-0296, Japan

^b D epartment of P hysics, Ochanomizu U niversity, Tokyo 112-8610, Japan

^c Institute of H um anities and S ciences,
 Ochanomizu U niversity, Tokyo 112-8610, Japan

^d D epartment of P hysics, Niigata U niversity, Niigata, 950-2128, Japan

A bstract

We study the sym m etric 2-zero texture of the neutrino m ass m atrix, which is obtained from the sym m etric Dirac neutrino m ass m atrix w ith 2-zeros and right-handed Majorana neutrino m ass m atrix w ith the general form via the see-saw m echanism , for the S U S Y S O (10) G U T m odel including the Pati-Salam sym m etry. We show that the only one texture in our m odel, having degenerate m ass spectrum for the 1st and 2nd generation of right-handed Majorana neutrino, can simultaneously explain the current neutrino experimental data, lepton flavor violating processes and baryon asym m etry of the U niverse. W ithin such a fram ework, the predicted values of the light and heavy Majorana neutrino m asses, together w ith J_{e3} , J_{CP} and $|M_{ee}|$, are almost uniquely determined.

¹E-mail address: bando@ aichi-u.ac.jp

²E-mail address: satoru@ phys.socha.ac.jp

³E-mail address: midori@ hep.phys.socha.ac.jp

⁴E-mail address: tanimoto@ m use.sci.niigata-u.ac.jp

1 Introduction

We have now come on information of neutrino masses and mixings [1]. Most remarkable one is that atmospheric neutrino mixing angle is almost maximal [2], while the solar neutrino mixing angle is large but not maximal [3, 4, 5], and further the ratio $m_{\text{sun}}^2 = m_{\text{atm}}^2$ is with ~ 0.2 , which is much different from the quark mass spectra. Having established such precise measurements of dominant neutrino oscillation parameters, the maximal-large mixing angles with mass hierarchy of order ~ 10 , we are now at a new stage of neutrino study. Our main concern is, not only how to reproduce the maximal-large mixing angles with less mass hierarchy but also how to predict the CP violating phases as well as the small U_{e3} [6].

Although there still remain many parameters of the neutrino mass matrix, we have already grasped its global structure. Thus, it is an important task to exhaust the candidates for the models which are compatible with the present neutrino data, producing quite naturally the maximal-large mixing angles as well as the mild hierarchical mass ratio, and to make very strict predictions of all the neutrino parameters. Then, we can make the criterions of realistic models clear and such models may be checked and selected by the near-future experiments.

It is well known that the following option for M_1 with M_d ⁵ (Georgi-Jarlskog type [7])

$$M_1 = \begin{pmatrix} 0 & 0 & a_d & 0 & 1 \\ 0 & 0 & 0 & 0 & 0 \\ 0 & 0 & 1 & 0 & 0 \\ 0 & 0 & 0 & 0 & 0 \\ 0 & 0 & 0 & 0 & 1 \end{pmatrix} \quad M_d = \begin{pmatrix} 0 & 0 & a_d & 0 & 1 \\ 0 & 0 & b_d & 0 & 0 \\ 0 & 0 & 1 & 0 & 0 \\ 0 & 0 & 0 & 0 & 0 \\ 0 & 0 & 0 & 0 & 1 \end{pmatrix} \quad (1.2)$$

can reproduce the beautiful relations between down quarks and charged leptons at the GUT scale,

$$m_d = m_b; \quad m_s = 3m_b; \quad m_e = \frac{m_d}{9}; \quad (1.3)$$

with the (1-2) mixing as $\sin \theta_{12}^{\text{CKM}} = \frac{1}{\sqrt{9}}$ [7]. Note that we need the "zero structure", namely some entries (the 1-1, 1-3 and 2-3 entries in this case) are far smaller than what we expect from naive hierarchical order of magnitudes⁶. Such zero textures are most popular and may be some indication of family symmetry.

Thus, we have seen an interesting fact, namely, the simplest GUT model works with an assumption that each element of the down quark Yukawa coupling is dominated by the contribution either from the 5 (10) or 45 (126) Higgs fields in $SU(5)$ ($SO(10)$) together with some further symmetry which guarantees the zero texture.

Encouraged by the above fact, we further try to examine whether such simple assumption can work in the up-quark and neutrino sectors. This may be one of the most hopeful

⁵This type of relation is realized if we assume that each element is dominated by either 5 (10) or 45 (126) in the $SU(5)$ ($SO(10)$) GUT, with concrete form is

$$M_1 = \begin{pmatrix} 0 & 0 & 5(10) & 0 & 1 \\ 0 & 0 & 45(126) & 0 & 0 \\ 0 & 0 & 0 & 5(10) & 0 \end{pmatrix} \quad (1.1)$$

⁶Otherwise the beautiful relations of eq. (1.3) are no more preserved because of the contribution of the 1-3 and 2-3 elements

approaches to make comparison of their predictions as definite as possible. In applying our GUT model, on the one hand, we need the information of the neutrino mass matrix M which is not directly obtained from M_u , since it is related with the Dirac neutrino mass matrix M_d via seesaw mechanism, $M = M_d^T M_R^{-1} M_d$, and we have some freedom coming from the right-handed neutrino mass matrix to determine which configuration of the Higgs representations should be chosen to give proper neutrino masses and mixings.

On the other hand, if the Nature demands the heavy Majorana masses for right-handed neutrinos to explain naturally the tiny neutrino masses via seesaw mechanism, the baryon number in the Universe may be affected by the leptogenesis which is caused by such heavy right-handed neutrino decay. Indeed the right-handed neutrino mass matrix plays a very important role in leptogenesis and it is considered one of the most hopeful scenarios to explain the origin of baryon number in the Universe, where the CP phases of the right-handed sector of neutrinos is very important. Combining the above information, what we should do next is to make definite predictions of various types of models which are compatible with the present experimental data, and to see what would be expected by including CP phases. In order to perform this, it is not enough to discuss the order of magnitude and we should make precise predictions based on strict theoretical arguments.

In the previous paper [8], we have shown that the 2-zero texture of quark mass matrices can reproduce the neutrino mass all-large mixing angles by connecting them to lepton mass matrices by the Pati-Salam GUT relation. There the group coefficient factors are important to reproduce solar neutrino data.

In this paper, we make a full analysis of such scenario of the SUSY SO(10) GUT model including the Pati-Salam symmetry and see how they are consistent with the neutrino masses and mixings as well as the baryon number in the Universe via leptogenesis, where the simplest form of right-handed neutrino mass matrix is slightly extended to more general cases within 2-zero texture, and study how they can be consistent with the neutrino oscillation data as well as the lepton flavor violation and leptogenesis.

In the section 2, the numerical analyses of masses and mixings are presented in the symmetric neutrino mass matrix with two zeros for the possible four textures of M_R . In sections 3 and 4, the lepton flavor violations and the leptogenesis are discussed in our model. Section 5 is devoted to summary.

2 Symmetric two-zero texture in neutrino mass matrix

2.1 The simplest form for M_R

First, let us consider the following symmetric 2-zero texture including the CP violating phases, which we have investigated previously [8];

$$M = \begin{pmatrix} 0 & & 0 & 1 & & 0 & & 0 & 1 \\ & 0 & & & & 0 & & 0 & \\ & & h & \bar{A} & m & = P & \begin{pmatrix} 0 & & 0 & 1 \\ & 0 & & 0 \\ & & e^i & \\ & & h & \bar{A} \\ & & 1 & \end{pmatrix} & P & m \end{pmatrix}; \quad (2.1)$$

where $'$, $0()$, $'$, $0(1)$, h , $0(1)$ and complex numbers, $;$ and h are converted to positive real numbers, $;$; h , by factoring out the phases with the diagonal phase matrix P ⁷. In such a texture, we examine how the parameters appearing in eq. (2.1) at the GUT scale are generally constrained from the present neutrino experimental data of $\sin^2 2_{\text{atm}}$; \tan^2_{sun} and the ratio of m_{sun}^2 to m_{atm}^2 . As usual we define the neutrino mixing angles which are expressed in terms of MNS matrix [9];

$$V_{\text{MNS}} = U_1^T U ; \quad (2.2)$$

where U_1 and U diagonalizes M_1 and M , respectively,

$$U_1^T M_1 U_1 = \text{diag}(m_e; m_\mu; m_\tau); \quad (2.3)$$

$$U^T M U = \text{diag}(m_e; m_\mu; m_\tau); \quad (2.4)$$

To make numerical calculation, we must take account of the contributions from the charged lepton side, U_1 in eq. (2.2). The complex symmetric charged lepton mass matrix is written in terms of the real symmetric matrix \overline{M}_1 ⁸

$$M_1 = P_1 \overline{M}_1 P_1; \quad (2.6)$$

where \overline{M}_1 is diagonalized to $\overline{M}_1^{\text{diag}}$ by real orthogonal matrix O_1 [10],

$$O_1^T \overline{M}_1 O_1 = \overline{M}_1^{\text{diag}}; \quad (2.7)$$

and, therefore, M_1 is diagonalized by $P_1 O_1$ as follows:

$$O_1^T P_1 M_1 P_1 O_1 = \overline{M}_1^{\text{diag}}; \quad (2.8)$$

Similarly, it is supposed that the Dirac and right-handed Majorana neutrino mass matrices are factored out the phases with the diagonal phase matrix P_D and P_R , respectively:

$$M_D = P_D \overline{M}_D P_D; \quad (2.9)$$

$$M_R = P_R \overline{M}_R P_R; \quad (2.10)$$

⁷This kind of 4-zero case has been studied extensively for the quark masses;

$$M_u = \begin{pmatrix} 0 & 0 & 1 \\ 0 & a_u & 0 \\ a_u & b_u & c_u \end{pmatrix} A m_t; \quad M_d = \begin{pmatrix} 0 & 0 & 1 \\ 0 & a_d & 0 \\ a_d & b_d & c_d \end{pmatrix} A m_b;$$

$$0 & c_u & 1 \\ 0 & c_d & 1 \end{pmatrix}$$

Here the matrix is assumed to be factored out all the phases by P in the 4-zero texture case. This is exactly possible in the case of 6-zero texture. Note that, however, we cannot factor out all the phases to make the matrix elements of M all real and there remains one phase as is seen in eq. (2.1). See Appendix A.

⁸Here, we take the following symmetric matrix with 2-zeros for \overline{M}_1 ,

$$\overline{M}_1 = \begin{pmatrix} 0 & p \frac{0}{m_e m} & p \frac{0}{m_e m} & 1 \\ p \frac{0}{m_e m} & 0 & p \frac{m}{m_e m} & p \frac{0}{m_e m} A \\ p \frac{m}{m_e m} & p \frac{m}{m_e m} & 0 & m \end{pmatrix}; \quad (2.5)$$

In general, one CP phase remains in this mass matrix, but its effect can be neglected as shown in Appendix B.

On the basis where the charged lepton mass matrix is diagonalized, the neutrino mass matrix at M_R scale is obtained from eq. (2.1)

$$\tilde{M}^f(M_R) = O_1^T Q^T \overline{M}^f(M_R) Q O_1; \quad (2.11)$$

where

$$\overline{M}^f(M_R) = \begin{pmatrix} 0 & 0 & 1 \\ \frac{B}{e} & e^i & h \frac{C}{A} m \\ 0 & h & 1 \end{pmatrix}; \quad (2.12)$$

$$Q = P P_1 = \begin{pmatrix} 0 & 0 & 1 \\ \frac{B}{e} & 0 & e^i \\ 0 & 0 & e^i \end{pmatrix} : \quad (2.13)$$

In order to compare our calculations with experimental results, we need the neutrino mass matrix at M_Z scale, which is obtained from the following one-loop RGE's relation between the neutrino mass matrices at M_Z and M_R [11];

$$\tilde{M}^f(M_Z) = \frac{0}{e} \frac{1}{1} \frac{0}{e} \frac{0}{1} \frac{1}{0} \frac{0}{A} \tilde{M}^f(M_R) \frac{0}{e} \frac{1}{1} \frac{0}{1} \frac{0}{0} \frac{1}{1} \frac{0}{A} : \quad (2.14)$$

Here \tilde{M}^f is the neutrino mass matrix on the basis where charged lepton mass matrix is diagonalized (see eq. (2.11)). The renormalization factors e and $\frac{1}{e}$ depend on the ratio of VEV's, $\tan \nu$. Here, we ignore the RGE effect from M_{GUT} to M_R scale considering that it almost does not change the values of masses for quarks and leptons. Using the form of eq. (2.14) we search the region of the parameter set $(\nu, h, \tan \nu, m_s, m_b)$ which are allowed by experimental data within 3% [1]:

$$\begin{aligned} 0.82 & \quad \sin^2 2_{\text{atm}}; \\ 0.28 & \quad \tan^2 \text{sun} \quad 0.64; \\ 0.73 & \quad 10^3 \quad m_{\text{atm}}^2 \quad 3.8 \quad 10^3 \text{eV}^2; \\ 5.4 & \quad 10^5 \quad m_{\text{sun}}^2 \quad 9.5 \quad 10^5 \text{eV}^2; \end{aligned} \quad (2.15)$$

In our model, we show that these two large mixing angles can be derived from symmetric four-zero texture with the Pati-Salam symmetry. We assume the following textures for up- and down-type quark mass matrices at the GUT scale [12],

$$M_d = \begin{pmatrix} 0 & 0 & q \frac{m_d m_s m_b}{m_b m_d} & 1 \\ q \frac{m_d m_s m_b}{m_b m_d} & r \frac{m_s}{m_d} & 0 & \frac{m_d m_b (m_b m_s m_d)}{m_b m_d} \\ 0 & \frac{m_d m_b (m_b m_s m_d)}{m_b m_d} & m_b & m_d \\ 0 & p \frac{m_d m_s}{m_b} & q \frac{0}{m_d} & 1 \\ p \frac{m_d m_s}{m_b} & q \frac{m_b}{m_d} & q \frac{m_d}{m_b} & m_b \end{pmatrix}, \quad (2.16)$$

Type	Texture				Type	Texture			
	0	0	126	0		0	0	126	0
S ₁	0	126	10	10 A	S ₂	0	0	126	0
	0	126	10	10 A		0	126	10	10 A
	0	10	126			0	10	10	
A ₁	0	0	126	0	A ₂	0	0	126	0
	0	126	126	126 A		0	126	126	126 A
	0	126	126			0	126	10	
A ₃	0	0	10	0	A ₄	0	0	10	0
	0	10	10	10 A		0	10	10	10 A
	0	10	126			0	10	10	
B ₁	0	0	10	0	B ₂	0	0	10	0
	0	10	126	126 A		0	10	126	126 A
	0	126	126			0	126	10	
C ₁	0	0	126	0	C ₄	0	0	126	0
	0	126	10	126 A		0	126	10	126 A
	0	126	126			0	126	10	
C ₂	0	0	10	0	C ₃	0	0	10	0
	0	10	10	126 A		0	10	10	126 A
	0	126	126			0	126	10	
F ₁	0	0	126	0	F ₄	0	0	126	0
	0	126	126	10 A		0	126	126	10 A
	0	10	126			0	10	10	
F ₂	0	0	10	0	F ₃	0	0	10	0
	0	10	126	10 A		0	10	126	10 A
	0	10	126			0	10	10	

Table 1: Classification of the up-type mass matrices, M_u and M_d .

which reproduces beautifully the down quark masses. For the up quark mass matrix, which is related to the Dirac neutrino mass matrix, we also take the following form

$$M_u = \begin{pmatrix} 0 & p \frac{m_u m_c}{m_t} & 1 \\ 0 & q \frac{m_u m_c}{m_t} & 0 \\ p \frac{m_u m_c}{m_t} & q \frac{m_u}{m_t} & 0 \end{pmatrix} ; \quad (2.17)$$

This, together with the form of eq. (2.16), reproduces all the observed quark masses as well as CKM mixing angles. As for M_d , it is well known that each element of M_u and M_d is dominated by the contribution either from 10 or 126 Higgs fields, where the ratio of Yukawa couplings of charged lepton to down quark are 1 or 3, respectively. More concretely, the following option for M_d (Georgi-Jarlskog type [7, 13, 14, 15])

$$M_d = \begin{pmatrix} 0 & 0 & 10 & 0 & 1 \\ 0 & 10 & 126 & 10 A & 0 \\ 0 & 126 & 10 & 10 A & 0 \\ 0 & 10 & 10 & 10 & 0 \end{pmatrix} ; \quad (2.18)$$

is known to reproduce very beautifully all the experimental data of m_b , m_s , m_d as well as m_b , m_s , m_d . On the other hand, M_u is related to M_d , which is not directly connected to

neutrino experiments, and we have not yet determined which configuration of the Higgs representations should be chosen to give proper neutrino masses and mixings. There are 16 types of textures for M_u , which are listed in Table 1. Once we fix their types, the Dirac neutrino mass matrix is automatically determined as

$$M_D = \begin{pmatrix} 0 & p \frac{m_u m_c}{m_t} & 1 & 0 & 0 & 1 & 0 & 0 & 1 \\ \bar{B} & 0 & \bar{q} \frac{m_u}{m_t} & \bar{C} & \bar{B} & \bar{q} & \bar{B} & \bar{a} & \bar{C} \\ \bar{q} & p \frac{m_u m_c}{m_t} & \bar{m}_t & \bar{C} & \bar{q} & \bar{m}_t & \bar{a} & \bar{b} & \bar{C} \\ \bar{m}_t & \bar{m}_c & \bar{A} & \bar{m}_t & \bar{B} & \bar{a} & \bar{b} & \bar{c} & \bar{A} \\ \bar{m}_c & \bar{m}_u & \bar{A} & \bar{A} & \bar{q} & \bar{m}_t & \bar{b} & \bar{c} & \bar{A} \\ 0 & \bar{q} \frac{m_t}{m_u} & \bar{A} & \bar{A} & \bar{0} & \bar{C} & \bar{a} & \bar{b} & \bar{C} \\ 0 & \bar{m}_u & \bar{A} & \bar{A} & \bar{0} & \bar{C} & \bar{c} & \bar{d} & \bar{A} \end{pmatrix}; \quad (2.19)$$

with the Clebsch-Gordan (CG) coefficients denoted by \bar{a} , \bar{b} , \bar{c} , \bar{d} , which are either 1 or -3, according to whether the Higgs representation is 10 or 126. For the right-handed Majorana mass matrix, to which only the 126 Higgs field couples, we assume the following simplest texture:

$$M_R = \begin{pmatrix} 0 & 1 & & \\ 0 & r & 0 & \\ \bar{B} & r & 0 & \bar{C} \\ 0 & 0 & 1 & \end{pmatrix} M_3; \quad (2.20)$$

with two real parameters M_3 and r . The neutrino mass matrix is now straightforwardly calculated as

$$M = M_D^T M_R^{-1} M_D = \begin{pmatrix} 0 & 0 & \frac{a^2}{r} & 0 & 1 \\ \bar{B} & \frac{a^2}{r} & 2 \frac{ab}{r} + c^2 & c(\frac{a}{r} + 1) \bar{C} & \frac{m_t^2}{M_3} \\ \bar{q} & \frac{a^2}{r} & \bar{r} & \bar{C} & \bar{A} \\ 0 & c(\frac{a}{r} + 1) & d^2 & d & \bar{A} \\ 0 & c(\frac{a}{r} + 1) & d^2 & d & \bar{A} \end{pmatrix}; \quad (2.21)$$

where a, b, c and d are defined in eq. (2.19). We know that the orders of the parameters in eq. (2.21) satisfy $a \approx b \approx c \approx 1$. In order to get a large mixing angle θ_{23} , the first term of the 2-3 element of M in eq. (2.21) should be of order d^2 , namely $ac \approx 0(d^2)$. This fixes the value of r as

$$r \approx \frac{ac}{d^2} \approx \frac{s \frac{m_u^2 m_c}{m_t^3}}{10^{(6-8)}}, \quad (2.22)$$

which is indeed the ratio of the the right-handed Majorana mass of the 3rd generation to those of the 1st and second generations. With this small r , M is approximately given by

$$M = \begin{pmatrix} 0 & 0 & \frac{a^2}{r} & 0 & 1 & 0 & 0 & 1 \\ \bar{B} & \frac{a^2}{r} & \frac{2ab}{r} & \bar{C} & \frac{m_t^2}{M_3} & \bar{B} & \bar{C} & \frac{d^2 m_t^2}{M_3} \\ \bar{q} & \frac{a^2}{r} & \frac{2ab}{r} & \bar{r} & \bar{C} & \bar{B} & \bar{C} & \bar{A} \\ 0 & \frac{a^2}{r} & \frac{2ab}{r} & \bar{r} & \bar{C} & \bar{B} & \bar{C} & \bar{A} \\ 0 & \frac{a^2}{r} & \frac{2ab}{r} & \bar{r} & \bar{C} & \bar{B} & \bar{C} & \bar{A} \\ 0 & \frac{a^2}{r} & \frac{2ab}{r} & \bar{r} & \bar{C} & \bar{B} & \bar{C} & \bar{A} \end{pmatrix}; \quad (2.23)$$

with

$$h = \frac{ac}{rd^2}; \quad = \frac{2ab}{rd^2}; \quad = \frac{a^2}{rd^2}; \quad (2.24)$$

where $h \approx 0(1)$. The forms of h , h and h are written in terms of m_t, m_c and m_u , with a parameter r , or equivalently h . In Table 2, we can classify the 16 types into five classes S, A, B, C and F. We have shown that the types belonging to a corresponding class yield the same predictions for mixing angles and masses [16].

Now, we can predict the values of m_u and m_c from the up-quark masses at the GUT scale,

$$m_u = 0.36 \quad 1.28 \text{ M eV}; \quad (2.25)$$

$$m_c = 209 \quad 300 \text{ M eV}; \quad (2.26)$$

$$m_t = 88 \quad 118 \text{ G eV}; \quad (2.27)$$

Type	d^2	r in ac=h unit	in $2m_c = \frac{P}{m_u m_t}$ unit	in $\frac{P}{m_c = m_t}$ unit
S_1	9	1=3	1	3
S_2	1	3	1	3
A_9	1	1	1	1
A_2	1	9	1	1
A_3	9	1=9	1	1
A_4	1	1	1	1
B_1	9	1=3	1	1=3
B_2	1	3	1	1=3
C_1	9	1	1=3	1
C_2	9	1=3	1=3	1=3
C_3	1	3	1=3	1=3
C_4	1	9	1=3	1=9
F_1	9	1=3	3	3
F_2	9	1=9	3	9
F_3	1	1	3	1
F_4	1	3	3	3

Table 2: The forms of h , and with the value of d for each type.

Type	\sin^2_{23}	\tan^2_{12}	m_{32}^2	m_{21}^2	m_1	m_2	m_3
S_1	0.42	0.43	0.28	3.8 10 3	5.4 10 5	0.0014	0.0075
S_2	0.43		0.28	3.8 10 3	5.4 10 5	0.0014	0.0075
Type	$j_{e3} j$	J_{CP}	$j M_{eeij}$	M_1	M_2	M_3	
S_1	0.010 0.025	(4.8 1.1) 10 3	0.019 0.024	1.1 10^9	1.1 10^9	3.0 10^{15}	
S_2	0.010	0	0.024	1.1 10^9	1.1 10^9	3.5 10^{14}	

Table 3: The allowed values for the neutrino observable in the types S_1 and S_2 . M_1 and M_2 are the masses for the 1st and 2nd generation of the right-handed Majorana neutrino.

which are obtained taking account of RGE's effect to the quark masses at the EW scale [17]. We have shown that the allowed region of and given by a neutrino mass matrix with two zeros in eq. (2.1) and the region of and for the five classes in our model, which are predicted from the up-quark masses at the GUT scale, are slightly separated on the $\{ \}$ plane, as seen in Figure 1. However, the light quark masses are ambiguous because of the non-perturbative QCD effect. Therefore, the allowed region of up quark mass, m_u , may be enlarged⁹. We obtained the overlapped region for the type S_1 (of the class S), as seen in Figure 4 of Ref. [8], enlarging the values of up quark mass at the GUT scale, $m_u = 0.36 - 2.56$ MeV. In the Table 2, we can see that the difference between the types S_1 and S_2 is only the scale of overall factor. For the type S_2 , we obtained the overlapped region, enlarging $m_u = 0.36 - 2.64$ MeV. Therefore, the type S_1 is the best type in the class S. We list the allowed values for the neutrino observable in the types S_1 and S_2 in the Table 3. The order of M_3 for S_1 is larger 1 order than S_2 . On the other hand, the values of

⁹The other possibility, that is, the effect of deviation from m_c in the 2-2 element of M_U , are discussed in Appendix C.

M_1 and M_2 are of the same order for both types.

In the next section, we will examine whether or not the general form of the right-handed Majorana neutrino mass matrix, which leads to the neutrino mass matrix with two zeros of eq. (2.1), can have parameter regions consistent with the neutrino experimental data, without enlarging the values of up quark mass at the GUT scale.

2.2 Including new parameters in M_R

2.2.1 Properties for the general form of M_R

Up to here, we have assumed the simplest form for M_R , having two parameters,

$$\text{Case I: } M_R = \begin{matrix} 0 & 0 & r & 0 \\ 0 & 0 & 0 & 1 \\ \hline B & r & 0 & 0 \\ 0 & 0 & 1 & C \end{matrix} M_3; \quad (2.28)$$

However, the actual case might have a general form which leads to the neutrino mass matrix with two zeros in eq. (2.1). Thus, we here include the new parameters s and t in M_R as follows:

$$M_R = \begin{matrix} 0 & 0 & r & 0 \\ 0 & 0 & 0 & 1 \\ \hline B & r & s & t \\ 0 & t & 1 & C \end{matrix} M_3; \quad (2.29)$$

where r , s and t are taken to be real. In order to clarify each effect of the new parameters, let us examine the above form, eq. (2.29) by dividing it into the following three cases:

$$\text{Case II: } M_R = \begin{matrix} 0 & 0 & r & 0 \\ 0 & 0 & 0 & 1 \\ \hline B & r & s & 0 \\ 0 & 0 & 1 & C \end{matrix} M_3; \quad (2.30)$$

$$\text{Case III: } M_R = \begin{matrix} 0 & 0 & 1 \\ 0 & 0 & 1 \\ \hline B & r & 0 \\ 0 & r & 0 & C \end{matrix} M_3; \quad (2.31)$$

$$\text{Case IV: } M_R = \begin{matrix} 0 & t & 1 \\ 0 & 0 & 1 \\ \hline B & r & s \\ 0 & r & 0 \\ 0 & t & 1 & C \end{matrix} M_3; \quad (2.32)$$

The final expression of the left-handed Majorana neutrino mass matrices for each case can be obtained via seesaw mechanism:

$$\text{Case I: } M = \begin{matrix} 0 & 0 & \frac{a^2}{r} & 0 & 1 \\ 0 & \frac{a^2}{r} & \frac{2ab}{r} + C^2 & \frac{ac}{r} + cd & \frac{m_t^2}{M_3} \\ \hline B & \frac{a^2}{r} & \frac{r}{r^2} & d^2 & \\ 0 & 0 & \frac{ac}{r} + cd & d^2 & \end{matrix}; \quad (2.33)$$

$$\text{Case II: } M = \begin{matrix} 0 & 0 & \frac{a^2}{r} & 0 & 1 \\ 0 & \frac{a^2}{r} & \frac{2ab}{r} & \frac{r^2}{r^2} s + C^2 & \\ \hline B & \frac{a^2}{r} & \frac{ac}{r} + cd & d^2 & \frac{m_t^2}{M_3} \\ 0 & 0 & \frac{ac}{r} + cd & d^2 & \end{matrix}; \quad (2.34)$$

$$\text{Case III : } M = \begin{bmatrix} 0 & 0 & \frac{a^2}{r} \\ \frac{B}{r} & \frac{a^2}{r} & \frac{2ab}{r} \\ 0 & \frac{ac}{r} & \frac{2ac}{r}t + \frac{a^2}{r^2}t^2 + c^2 \end{bmatrix} \begin{matrix} 0 \\ 0 \\ 0 \end{matrix} \begin{matrix} 1 \\ \frac{m_t^2}{M_3} \\ \frac{m_t^2}{M_3} \end{matrix}; \quad (2.35)$$

$$\text{Case IV : } M = \begin{bmatrix} 0 & 0 & \frac{a^2}{r} \\ \frac{B}{r} & \frac{a^2}{r} & \frac{2ab}{r} \\ 0 & \frac{ac}{r} & \frac{2ac}{r}t + \frac{a^2}{r^2}t^2 + c^2 \end{bmatrix} \begin{matrix} 0 \\ 0 \\ 0 \end{matrix} \begin{matrix} 1 \\ \frac{m_t^2}{M_3} \\ \frac{m_t^2}{M_3} \end{matrix}; \quad (2.36)$$

As is seen from the above expressions, the parameter s affects only on the 2-2 element of M , and the additional contribution to the 2-3 element comes only from the parameter t . In eqs. (2.33) and (2.34), we found that the 2-3 element of M in the case II is the same as that in the case I, namely, the condition for getting a large mixing angle θ_{23} in the case II is the same as that in the case I. On the other hand, the condition for the case III is, similarly, the same as that in the case IV. Note that the 1-2 element of M has the same form in all cases.

For each case, we will search for the parameter regions, which are allowed by the experimental data within $\pm 3\%$, and show that, in the case II, the types S_1 and S_2 have the allowed regions, the types C_1, F_3 and F_4 in the case III, and the types $S_1, S_2, A_1, B_1, C_1, F_3$ and F_4 in the case IV.

2.2.2 Case II

First, let us examine the case II. Since a new parameter, s , affects only on the 2-2 element of M , namely, the allowed regions for the classes S, A, B, C and F in the case I, as depicted in Figure 1, can be enlarged only in the direction of s . The first term in the 2-2 element becomes comparable with the second term at the following value of s :

$$\frac{2ab}{r}, \frac{a^2s}{r^2} \approx s, \frac{2br}{a} \approx 5 \times 10^7; \quad (2.37)$$

Thus, the difference between the region of s in the case I and the case II is appreciable around this value of s . We obtained the overlapped region in the types S_1 and S_2 with $h = 1.3$, as depicted in Figure 2 and 3. It is shown that the region which is consistent with the experimental data has now been focused only on the narrow region. The typical values for these types are listed in Table 4, where the values at the maximum and minimum value of θ_{e3} are written. In this table, as we have expected, we find that the overlapped regions can be obtained around $s = 10^{16-17}$. The predicted values of θ_{e3} is given

$$\theta_{e3} = 0.014 \quad 0.071; \quad (2.38)$$

for the type S_1 , and

$$\theta_{e3} = 0.013 \quad 0.016; \quad (2.39)$$

for the type S_2 .

Type	S_1^{max}	S_1^{min}	S_2^{max}	S_2^{min}
$\mathbf{jU}_{e3}\mathbf{j}$	0.071	0.014	0.016	0.013
	0.0	0.0	0.0	0.0
	5 =8			
\mathbf{jM}_{eeij}	0.022	0.027	0.029	0.027
J_{CP}	0.01	0.0	0.0	0.0
m_1 (eV)	$1.7 \cdot 10^{-3}$	$1.4 \cdot 10^{-3}$	$1.4 \cdot 10^{-3}$	$1.4 \cdot 10^{-3}$
m_2 (eV)	$7.9 \cdot 10^{-3}$	$7.5 \cdot 10^{-3}$	$7.8 \cdot 10^{-3}$	$7.5 \cdot 10^{-3}$
m_3 (eV)	$5.8 \cdot 10^{-2}$	$5.8 \cdot 10^{-2}$	$5.8 \cdot 10^{-2}$	$5.9 \cdot 10^{-2}$
$\sin^2 \theta_{23}$	0.45	0.43	0.44	0.43
$\tan^2 \theta_{12}$	0.29	0.29	0.28	0.28
m_{32}^2 (eV ²)	$3.3 \cdot 10^{-3}$	$3.3 \cdot 10^{-3}$	$3.3 \cdot 10^{-3}$	$3.4 \cdot 10^{-3}$
m_{21}^2 (eV ²)	$6.0 \cdot 10^{-5}$	$5.4 \cdot 10^{-5}$	$5.9 \cdot 10^{-5}$	$5.5 \cdot 10^{-5}$
m_u (MeV)	0.56	0.52	1.04	1.00
m_c (MeV)	300	230	300	280
m_t (GeV)	88	88	108	108
s	$1.0 \cdot 10^{-6}$	$6.5 \cdot 10^{-7}$	$7.0 \cdot 10^{-6}$	$6.0 \cdot 10^{-6}$
M_1 (GeV)	$2.7 \cdot 10^7$	$2.7 \cdot 10^7$	$9.6 \cdot 10^7$	$9.6 \cdot 10^7$
M_2 (GeV)	$3.0 \cdot 10^9$	$2.0 \cdot 10^9$	$3.6 \cdot 10^9$	$3.1 \cdot 10^9$
M_3 (GeV)	$3.0 \cdot 10^{15}$	$3.0 \cdot 10^{15}$	$5.0 \cdot 10^{14}$	$5.0 \cdot 10^{14}$

Table 4: Results of numerical calculations for S_1 and S_2 in the case II. The values at the maximum and minimum value of $\mathbf{jU}_{e3}\mathbf{j}$ are written.

2.2.3 Case III

Next, we discuss the case III, in which the form of the 2-3 element of M is different from the one in the case I. We have listed the condition for getting a large θ_{23} of each class in Table 5. Here, a new parameter t is included in the condition of r . Therefore, the allowed region for five classes, as seen in Figure 1, can be enlarged both in direction of r and t . The first term in the 2-3 element becomes comparable with the second term at the following value of t :

$$\frac{ac}{r}, \frac{ad}{r}t! \quad t' \quad \frac{c}{d} \quad 4 \quad 2 \quad 10^3: \quad (2.40)$$

Thus, the difference between the region of r and t in the case I and the case III is appreciable around this value of t . We show that the types C_1, F_3 and F_4 provide the overlapped region as depicted in Figure 4, 5 and 6. The typical values of C_1, F_3 and F_4 are listed in Table 6. In similar to the case II, as we have expected, we find that the overlapped regions can be obtained around $t = 10^3$. Then, the predicted values of $\mathbf{jU}_{e3}\mathbf{j}$ is given for the type C_1 ,

$$\mathbf{jU}_{e3}\mathbf{j} = 0.025; \quad (2.41)$$

for the type F_3 ,

$$\mathbf{jU}_{e3}\mathbf{j} = 0.059 \quad 0.17; \quad (2.42)$$

and for the type F_4 ,

$$\mathbf{jU}_{e3}\mathbf{j} = 0.19; \quad (2.43)$$

Type	condition	Type	condition
S_1	$r' \frac{a(c+3t)}{3h+c}$	S_2	$r' \frac{3a(c-t)}{h-c}$
A_1	$r' \frac{a(c-t)}{h-c}$	A_2	$r' \frac{3a(3c+t)}{h+3c}$
A_3	$r' \frac{a(c+3t)}{3(3h+3c)}$	A_4	$r' \frac{a(c-t)}{h-c}$
B_1	$r' \frac{a(c-t)}{3(h-c)}$	B_2	$r' \frac{a(3c+t)}{h+3c}$
C_1	$r' \frac{a(c-t)}{h-c}$	C_2	$r' \frac{a(c-t)}{3(h-c)}$
C_3	$r' \frac{a(3c+t)}{h+3c}$	C_4	$r' \frac{3a(3c+t)}{h+3c}$
F_1	$r' \frac{a(c+3t)}{3h+c}$	F_2	$r' \frac{a(c+3t)}{3(3h+c)}$
F_3	$r' \frac{a(c-t)}{h-c}$	F_4	$r' \frac{3a(c-t)}{h-c}$

Table 5: The condition for getting a large $|r_{23}|$ in the case III and IV .

The types C_1 and F_4 have very narrow region. On the other hand, wide region is obtained in the type F_3 .

2.2.4 Case IV

Finally, we consider the most general case for M_R , which includes two new parameters, s and t . In this case, because eq. (2.36) includes both eqs. (2.34) and (2.35), we can expect that $S_1; S_2$, which are allowed in the case II, and $C_1; F_3; F_4$, which are allowed in the case III, have the overlapped region. By numerical calculations, we have confirmed that A_1 and B_1 also provide the overlapped regions as depicted in Figures 7 – 13. The typical values of these seven types are listed in Table 7, 8 and 9. We present the predicted values of $|J_{e3}|$ for seven types as follows:

$$|J_{e3}| = 0.014 \quad 0.027 \quad (\text{Type } S_1); \quad (2.44)$$

$$|J_{e3}| = 0.021 \quad 0.199 \quad (\text{Type } S_2); \quad (2.45)$$

$$|J_{e3}| = 0.032 \quad 0.17 \quad (\text{Type } A_1); \quad (2.46)$$

$$|J_{e3}| = 0.049 \quad 0.11 \quad (\text{Type } B_1); \quad (2.47)$$

$$|J_{e3}| = 0.012 \quad (\text{Type } C_1); \quad (2.48)$$

$$|J_{e3}| = 0.056 \quad 0.199 \quad (\text{Type } F_3); \quad (2.49)$$

$$|J_{e3}| = 0.17 \quad (\text{Type } F_4); \quad (2.50)$$

In conclusion, the prediction of $|J_{e3}|$ depends on the types of Dirac neutrino mass matrix and right-handed Majorana mass matrix considerably.

3 Lepton flavor violations : $e_j \neq e_i$

In the model of MSSM with right-handed neutrinos, lepton flavor violations (LFV) are induced through the renormalization group effects to the slepton mixings and the predicted

Type	C_1	F_3^{\max}	F_3^{\min}	F_4
$\mathcal{U}_{e3}j$	0.025	0.17	0.059	0.19
	0.0	=8	=8	=8
	=8	=2	=8	3 =4
\mathcal{M}_{eeij}	0.019	0.027	0.084	0.57
J_{CP}	0.0042	0.033	0.005	0.031
m_1 (eV)	$1.4 \cdot 10^{-3}$	$3.1 \cdot 10^{-3}$	$1.6 \cdot 10^{-3}$	$5.7 \cdot 10^{-3}$
m_2 (eV)	$7.5 \cdot 10^{-3}$	$9.6 \cdot 10^{-3}$	$8.3 \cdot 10^{-3}$	$9.9 \cdot 10^{-3}$
m_3 (eV)	$6.2 \cdot 10^{-2}$	$4.4 \cdot 10^{-2}$	$3.7 \cdot 10^{-2}$	$4.4 \cdot 10^{-2}$
\sin^2_{23}	0.46	0.45	0.49	0.30
\tan^2_{12}	0.28	0.40	0.29	0.56
m_{32}^2 (eV ²)	$3.8 \cdot 10^{-3}$	$1.9 \cdot 10^{-3}$	$1.3 \cdot 10^{-3}$	$1.8 \cdot 10^{-3}$
m_{21}^2 (eV ²)	$5.5 \cdot 10^{-5}$	$8.2 \cdot 10^{-5}$	$6.7 \cdot 10^{-5}$	$6.6 \cdot 10^{-5}$
m_u (MeV)	0.48	1.2	1.24	1.12
m_c (MeV)	290	300	220	220
m_t (GeV)	92	93	88	113
t	$1.4 \cdot 10^{-3}$	$3.0 \cdot 10^{-3}$	$3.0 \cdot 10^{-3}$	$2.5 \cdot 10^{-3}$
M_1 (GeV)	$1.2 \cdot 10^7$	$4.7 \cdot 10^5$	$6.5 \cdot 10^5$	$6.2 \cdot 10^6$
M_2 (GeV)	$6.1 \cdot 10^9$	$4.5 \cdot 10^9$	$4.5 \cdot 10^9$	$5.6 \cdot 10^9$
M_3 (GeV)	$3.09 \cdot 10^{15}$	$5.0 \cdot 10^{14}$	$5.0 \cdot 10^{14}$	$9.0 \cdot 10^{14}$

Table 6: Results of numerical calculations for C_1 ; F_3 and F_4 in the case III. The values at the maximum and minimum value of $\mathcal{U}_{e3}j$ are written.

Type	S_1^{\max}	S_1^{\min}	S_2^{\max}	S_2^{\min}
$\mathcal{U}_{e3}j$	0.027	0.014	0.19	0.021
	0.0	0.0	=8	0.0
	7 =8		=4	0.0
\mathcal{M}_{eeij}	0.024	0.027	0.27	0.034
J_{CP}	$4.0 \cdot 10^{-3}$	0.0	0.034	0.0
m_1 (eV)	$1.5 \cdot 10^{-3}$	$1.4 \cdot 10^{-3}$	$4.3 \cdot 10^{-3}$	$1.7 \cdot 10^{-3}$
m_2 (eV)	$7.6 \cdot 10^{-3}$	$7.6 \cdot 10^{-3}$	$9.1 \cdot 10^{-3}$	$7.5 \cdot 10^{-3}$
m_3 (eV)	$5.8 \cdot 10^{-2}$	$5.8 \cdot 10^{-2}$	$5.0 \cdot 10^{-2}$	$5.9 \cdot 10^{-2}$
\sin^2_{23}	0.44	0.43	0.38	0.46
\tan^2_{12}	0.29	0.28	0.39	0.35
m_{32}^2 (eV ²)	$3.3 \cdot 10^{-3}$	$3.3 \cdot 10^{-3}$	$2.4 \cdot 10^{-3}$	$3.4 \cdot 10^{-3}$
m_{21}^2 (eV ²)	$5.5 \cdot 10^{-5}$	$5.5 \cdot 10^{-5}$	$6.4 \cdot 10^{-5}$	$5.4 \cdot 10^{-5}$
m_u (MeV)	1.28	0.52	0.96	0.48
m_c (MeV)	280	290	270	280
m_t (GeV)	88	88	93	108
s	$1.0 \cdot 10^{-6}$	$1.0 \cdot 10^{-6}$	$8.0 \cdot 10^{-6}$	$6.0 \cdot 10^{-6}$
t	$1.0 \cdot 10^{-4}$	$1.0 \cdot 10^{-4}$	$2.0 \cdot 10^{-3}$	$4.0 \cdot 10^{-3}$
M_1 (GeV)	$1.5 \cdot 10^8$	$2.9 \cdot 10^7$	$2.9 \cdot 10^7$	$1.1 \cdot 10^7$
M_2 (GeV)	$3.1 \cdot 10^9$	$3.0 \cdot 10^9$	$2.0 \cdot 10^9$	$5.0 \cdot 10^9$
M_3 (GeV)	$3.0 \cdot 10^{15}$	$3.0 \cdot 10^{15}$	$5.0 \cdot 10^{14}$	$5.0 \cdot 10^{14}$

Table 7: Results of numerical calculations for S_1 and S_2 in the case IV. The values at the maximum and minimum value of $\mathcal{U}_{e3}j$ are written.

Type	A_1^{max}	A_1^{min}	B_1^{max}	B_1^{min}
$j_{e3}j$	0.17	0.032	0.11	0.049
	0.0	0.0	0.0	0.0
		0.0	=2	0.0
jM_{eeij}	0.24	0.049	0.096	0.075
J_{CP}	0.01	0.0	0.012	0.0
m_1 (eV)	$3.6 \cdot 10^{-3}$	$1.6 \cdot 10^{-3}$	$1.9 \cdot 10^{-3}$	$1.9 \cdot 10^{-3}$
m_2 (eV)	$8.6 \cdot 10^{-3}$	$8.4 \cdot 10^{-3}$	$8.5 \cdot 10^{-3}$	$8.5 \cdot 10^{-3}$
m_3 (eV)	$6.0 \cdot 10^{-2}$	$5.1 \cdot 10^{-2}$	$4.7 \cdot 10^{-2}$	$4.7 \cdot 10^{-2}$
\sin^2_{23}	0.42	0.48	0.48	0.49
\tan^2_{12}	0.40	0.31	0.29	0.37
m_{32}^2 (eV ²)	$3.5 \cdot 10^{-3}$	$2.6 \cdot 10^{-3}$	$2.1 \cdot 10^{-3}$	$2.1 \cdot 10^{-3}$
m_{21}^2 (eV ²)	$6.2 \cdot 10^{-5}$	$6.7 \cdot 10^{-5}$	$6.8 \cdot 10^{-5}$	$6.8 \cdot 10^{-5}$
m_u (MeV)	0.36	0.44	0.8	0.8
m_c (MeV)	210	260	300	300
m_t (GeV)	113	108	103	103
s	$3.0 \cdot 10^{-6}$	$4.0 \cdot 10^{-6}$	$8.0 \cdot 10^{-6}$	$8.0 \cdot 10^{-6}$
t	$1.5 \cdot 10^{-3}$	$1.5 \cdot 10^{-3}$	$3.0 \cdot 10^{-3}$	$3.0 \cdot 10^{-3}$
M_1 (GeV)	$1.9 \cdot 10^6$	$4.4 \cdot 10^6$	$3.5 \cdot 10^5$	$3.5 \cdot 10^5$
M_2 (GeV)	$3.8 \cdot 10^9$	$8.8 \cdot 10^9$	$5.0 \cdot 10^9$	$5.0 \cdot 10^9$
M_3 (GeV)	$5.0 \cdot 10^{15}$	$5.0 \cdot 10^{15}$	$5.0 \cdot 10^{15}$	$5.0 \cdot 10^{15}$

Table 8: Results of numerical calculations for A_1 and B_1 in the case IV. The values at the maximum and minimum value of $j_{e3}j$ are written.

branching ratios of the processes can be comparable with the current experimental upper bound [18, 19, 20, 21, 22, 23, 24] :

$$Br(\bar{e} \rightarrow e) < 1.2 \cdot 10^{-11} \quad [25]; \quad (3.1)$$

$$Br(\bar{e} \rightarrow e) < 3.6 \cdot 10^{-7} \quad [26]; \quad (3.2)$$

$$Br(\bar{e} \rightarrow e) < 3.1 \cdot 10^{-7} \quad [27]; \quad (3.3)$$

Therefore, we have to examine these decay rates carefully in our model.

Let us start with writing down the leptonic parts of soft SUSY breaking terms as follows:

$$L_{\text{soft}} = (m_L^2)_{ij} \tilde{L}_i^Y \tilde{L}_j + (m_e^2)_{ij} \tilde{e}_R i \tilde{e}_R j + (m_{\tilde{\nu}}^2)_{ij} \tilde{\nu}_R i \tilde{\nu}_R j + (A_e)_{ij} H_d \tilde{e}_R i \tilde{L}_j + (A_u)_{ij} H_u \tilde{\nu}_R i \tilde{L}_j; \quad (3.4)$$

where \tilde{L}_i ; $\tilde{e}_R i$ and $\tilde{\nu}_R i$ are the supersymmetric scalar partner of left-handed lepton doublet, right-handed lepton singlet and right-handed neutrino, $(m_L^2)_{ij}$; $(m_e^2)_{ij}$ and $(m_{\tilde{\nu}}^2)_{ij}$ are the 3 3 hermitian slepton mass matrices, $(A_e)_{ij}$ and $(A_u)_{ij}$ are trilinear couplings of Higgs doublets H_u ; H_d and sleptons, respectively (A-term). H_u and H_d couple to neutrinos and charged leptons, respectively. Non-vanishing off-diagonal elements of slepton mass matrices become the new source of LFV .

In minimal supergravity (mSUGRA) models, it is assumed that the slepton mass matrices are diagonal and have common mass scale m_0 at the GUT scale, and that the trilinear couplings are proportional to Yukawa couplings:

$$(m_L^2)_{ij} = (m_e^2)_{ij} = (m_{\tilde{\nu}}^2)_{ij} = \tilde{m}_0^2; \quad m_{H_d}^2 = m_{H_u}^2 = m_0^2; \\ A_u = Y_u m_0; \quad A_e = Y_e m_0; \quad (3.5)$$

Type	C_1	F_3^{max}	F_3^{min}	F_4^{max}	F_4^{min}
$J_{e3}j$	0.012	0.19	0.056	0.19	0.17
	0.0	=8	0.0	0.0	=8
	0.0	3 =4	0.0		7 =8
$J_{M_{ee}ij}$	0.025	0.35	0.089	0.67	0.51
J_{CP}	0.0	0.034	0.0	0.0	0.031
m_1 (eV)	$1.4 \cdot 10^{-3}$	$2.9 \cdot 10^{-3}$	$1.6 \cdot 10^{-3}$	$5.5 \cdot 10^{-3}$	$5.6 \cdot 10^{-3}$
m_2 (eV)	$7.5 \cdot 10^{-3}$	$8.6 \cdot 10^{-3}$	$7.5 \cdot 10^{-3}$	$1.1 \cdot 10^{-2}$	$9.9 \cdot 10^{-3}$
m_3 (eV)	$6.1 \cdot 10^{-2}$	$4.0 \cdot 10^{-2}$	$3.7 \cdot 10^{-2}$	$3.9 \cdot 10^{-2}$	$4.3 \cdot 10^{-2}$
$\sin^2 \theta_{23}$	0.46	0.44	0.50	0.39	0.30
$\tan^2 \theta_{12}$	0.28	0.35	0.35	0.56	0.59
m_{32}^2 (eV ²)	$3.7 \cdot 10^{-3}$	$1.5 \cdot 10^{-3}$	$1.3 \cdot 10^{-3}$	$1.4 \cdot 10^{-3}$	$2.2 \cdot 10^{-3}$
m_{21}^2 (eV ²)	$5.5 \cdot 10^{-5}$	$6.6 \cdot 10^{-5}$	$5.4 \cdot 10^{-5}$	$9.4 \cdot 10^{-5}$	$6.7 \cdot 10^{-5}$
m_u (MeV)	0.88	1.12	1.24	1.12	1.2
m_c (MeV)	300	290	210	210	210
m_t (GeV)	88	88	88	113	118
s	$3.2 \cdot 10^{-7}$	$2.0 \cdot 10^{-7}$	$4.0 \cdot 10^{-7}$	$4.0 \cdot 10^{-7}$	$1.0 \cdot 10^{-7}$
t	$1.9 \cdot 10^{-3}$	$3.0 \cdot 10^{-3}$	$3.0 \cdot 10^{-3}$	$2.5 \cdot 10^{-3}$	$2.5 \cdot 10^{-3}$
M_1 (GeV)	$2.8 \cdot 10^7$	$4.5 \cdot 10^5$	$6.5 \cdot 10^5$	$6.3 \cdot 10^6$	$6.7 \cdot 10^6$
M_2 (GeV)	$9.4 \cdot 10^9$	$4.4 \cdot 10^9$	$4.3 \cdot 10^9$	$5.3 \cdot 10^9$	$5.5 \cdot 10^9$
M_3 (GeV)	$2.85 \cdot 10^{15}$	$5.0 \cdot 10^{14}$	$5.0 \cdot 10^{14}$	$9.0 \cdot 10^{14}$	$9.0 \cdot 10^{14}$

Table 9: Results of numerical calculations for C_1 ; F_3 and F_4 in the case IV. The values at the maximum and minimum value of $J_{e3}j$ are written.

and the same conditions are assumed in quark sector. The mass of supersymmetric fermion partner of gauge bosons (gauginos) are also fixed to be $M_{1=2}$ at the GUT scale. Even if no sources of LFV are assumed at the GUT scale, the LFV will be induced in slepton mass matrix through renormalization of Yukawa and gauge interactions. The one-loop renormalization group equation (RGE) for left-handed slepton mass matrix is given by

$$\frac{d}{d} (m_L^2)_{ij} = \frac{d}{d} (m_L^2)_{ij} \Big|_{M_{\text{SSM}}} + \frac{1}{16} \frac{h}{2} (m_L^2 Y^Y Y + Y^Y Y m_L^2)_{ij} + 2 (Y^Y m_{\tilde{Y}} + m_{H_u}^2 Y^Y Y + A^Y A)_{ij}^i ; \quad (3.6)$$

where the first term is the MSSM term which is lepton flavor conserving, while the second term contains the source of LFV, Y is the neutrino Yukawa coupling matrix ($= M_D = v_u$).

It is easy to see in eq. (3.6) that the Yukawa coupling of the neutrino contributes to the LFV. Assuming the boundary conditions of eq. (3.5), we obtain the leading log approximation for the off-diagonal elements of left-handed slepton mass matrix at the scale of right-handed neutrino masses as follows [19, 20, 24]:

$$(m_L^2)_{ij} \sim \frac{1}{8} (3m_0^2 + a_0^2) H_{ij} ; \quad (3.7)$$

where the matrix H_{ij} is defined by

$$H_{ij} = \overline{(Y^Y L Y)}_{ij} ; \quad L = \text{diag} \ln \frac{M_{\text{GUT}}}{M_1} ; \ln \frac{M_{\text{GUT}}}{M_2} ; \ln \frac{M_{\text{GUT}}}{M_3} ; \quad (3.8)$$

where \bar{Y} is the neutrino Yukawa coupling matrix on the basis where the charged lepton and right-handed Majorana mass matrix is diagonal. The branching ratio for the LFV processes: $e_j \rightarrow e_i$ is approximately given by

$$Br(e_j \rightarrow e_i) \sim \frac{3}{G_F^2} \frac{|(m^2_{ij})_{ij}|^2}{m_S^8} \tan^2 \theta_W ; \quad (3.9)$$

where m_S is the typical mass scale of superparticles, $\theta_W = 128^\circ$ and G_F is the Fermi coupling constant, respectively. The excellent approximation of m_S to the exact RGE result is given by [28]

$$m_S^8 \sim 0.5 m_0^2 M_{1=2}^2 (m_0 + 0.6 M_{1=2})^2 ; \quad (3.10)$$

It is clear that the element H_{12} , H_{13} and H_{23} dominantly contribute to the processes of $e_j \rightarrow e_i$, $e_j \rightarrow e_i$ and $e_j \rightarrow e_i$, respectively.

Let us calculate the matrix H_{ij} in our model. The \bar{Y} is given by

$$\bar{Y} = O_R Y O_L ; \quad (3.11)$$

where matrix O_R and O_L are the orthogonal matrices which diagonalize the right-handed Majorana mass matrix and charged lepton mass matrix, respectively. Then, the matrix H_{ij} is given by

$$H_{ij} = (O_L^T Y^T O_R^T)_{ik} L_k (O_R Y O_L)_{kj} ; \quad (3.12)$$

For the case I, matrix O_R is given by

$$O_R = \begin{pmatrix} 0 & 1 & 1 & 0 & 1 \\ 1 & 0 & 0 & 1 & 0 \\ 1 & 0 & 0 & 0 & 1 \\ 0 & 1 & 0 & 0 & 1 \end{pmatrix} ; \quad (3.13)$$

then we obtain the formulae of H_{ij} assuming the type S_1 for neutrino Yukawa coupling matrix which is the mostly allowed one :

$$H_{12} \sim a^2 (O_{11}O_{12} + O_{12}O_{11}) + (bO_{121} + cO_{131}) (bO_{122} + cO_{132}) + a f b (O_{113}O_{121} + O_{111}O_{122}) + c (O_{112}O_{131} + O_{111}O_{132}) g \ln \frac{M_{GUT}}{M_1} + (cO_{112} + dO_{131}) (cO_{122} + dO_{132}) \ln \frac{M_{GUT}}{M_3} ; \quad (3.14)$$

$$H_{13} \sim a^2 (O_{11}O_{13} + O_{13}O_{11}) + (bO_{121} + cO_{131}) (bO_{123} + cO_{133}) + a f b (O_{113}O_{121} + O_{111}O_{123}) + c (O_{113}O_{131} + O_{111}O_{133}) g \ln \frac{M_{GUT}}{M_1} + (cO_{121} + dO_{131}) (cO_{123} + dO_{133}) \ln \frac{M_{GUT}}{M_3} ; \quad (3.15)$$

$$H_{23} \sim a^2 (O_{12}O_{13} + O_{13}O_{12}) + (bO_{122} + cO_{132}) (bO_{123} + cO_{133}) + a f b (O_{113}O_{122} + O_{112}O_{123}) + c (O_{113}O_{132} + O_{112}O_{133}) g \ln \frac{M_{GUT}}{M_1} + (cO_{122} + dO_{132}) (cO_{123} + dO_{133}) \ln \frac{M_{GUT}}{M_3} ; \quad (3.16)$$

where we have used the mass spectrum for the case I: $M_1 = M_2$. In the following calculations of branching ratios, the relations: $a = 3a_e$; $b = b_e$; $c = c_e$; $d = 3d_e$ for the type S_1 and $a = 3a_e$; $b = b_e$; $c = c_e$; $d = d_e$ for the type S_2 will be taken. The orthogonal mass matrix O_1 is approximately given by [12]

$$O_1 = \begin{pmatrix} 0 & q \frac{m_e}{m} & r \frac{m_e^2 m}{m^3} & 1 \\ \bar{B} & 1 & q \frac{m_e}{m} & 0 \\ \bar{B} & q \frac{m_e}{m} & 1 & q \frac{m_e}{m} \\ \bar{C} & r \frac{m_e^2}{m^2} & q \frac{m_e}{m} & 1 \end{pmatrix} = \begin{pmatrix} 0 & 1 & " & 1 \\ \bar{B} & " & 1 & \bar{C} \\ \bar{B} & " & 1 & \bar{C} \\ \bar{A} & " & 1 & 1 \end{pmatrix}; \quad \begin{pmatrix} s \frac{m_e}{m} \\ s \frac{m_e}{m} \end{pmatrix}; \quad \begin{pmatrix} s \frac{m_e}{m} \\ s \frac{m_e}{m} \end{pmatrix} \quad (3.17)$$

Under the above parametrization, we can calculate the off-diagonal elements of mass matrix H_{ij} :

$$H_{12} j' = ab \ln \frac{M_{GUT}}{M_1} \quad b" \ln \frac{M_{GUT}}{M_1} \quad d^2" \ln \frac{M_{GUT}}{M_3} \quad d^2" \ln \frac{M_{GUT}}{M_3}; \quad (3.18)$$

$$H_{13} j' = ac \ln \frac{M_{GUT}}{M_1} \quad bc" \ln \frac{M_{GUT}}{M_1} + d^2" \ln \frac{M_{GUT}}{M_3} \quad d^2" \ln \frac{M_{GUT}}{M_3}; \quad (3.19)$$

$$H_{23} j' = cd \ln \frac{M_{GUT}}{M_3} \quad c" \ln \frac{M_{GUT}}{M_1} + d^2" \ln \frac{M_{GUT}}{M_3} \quad d^2" \ln \frac{M_{GUT}}{M_3}; \quad (3.20)$$

where the terms including the charged lepton mixing matrix are dominant ones. These formulae provide the following relations of branching ratios:

$$Br(\bar{e} \rightarrow e) < Br(\bar{\nu}_e \rightarrow e) < Br(\bar{\nu}_e \rightarrow \nu_e); \quad (3.21)$$

for the type S_1 and S_2 . For the case II, III and IV, the predicted branching ratios are almost the same as the case I. Numerical calculations of the branching ratios using the leading log approximation (eqs. (3.7), (3.8), (3.9) and (3.10)) of $\bar{e} \rightarrow e$, $\bar{\nu}_e \rightarrow e$ and $\bar{\nu}_e \rightarrow \nu_e$ are presented in Figure 14, 15 and 16, respectively¹⁰. In these figures, the branching ratios are scatter plotted in the region of $m_0 = 100 \text{--} 1000 \text{ GeV}$, $M_{1=2} = 100 \text{--} 1000 \text{ GeV}$ and $\tan \theta = 5 \text{--} 50$ for each processes. The a is fixed to be $a_0 = 0$.

As seen in these figures, the branching ratios of all processes are safely predicted below the current experimental upper bounds. The predicted branching ratios for the type S_2 are lower almost one order of magnitude than the one for the type S_1 . This is due to the differences in CG coefficients in 3-3 elements of neutrino Yukawa coupling matrix. Only

$\bar{\nu}_e \rightarrow \nu_e$ process for the type S_1 may be observed in the future experiments in which the sensitivity will reach to be $Br(\bar{\nu}_e \rightarrow \nu_e) \sim 10^9$ [29]. The predicted branching ratios of

$\bar{\nu}_e \rightarrow \nu_e$ process for the type S_2 and the other processes for both types are too small to be observed even in the future experiments.

4 Thermal Leptogenesis

In this section, we discuss the calculation of baryon asymmetry of the universe based on the leptogenesis scenario [30] for our textures. In the leptogenesis scenario, lepton asymmetry

¹⁰Note that this approximation deviates significantly from exact RGE result in the region of large $M_{1=2}$ and small m_0 [28]. However, this deviations are at most of a factor ~ 10 . For $m_0 = 100 \text{ GeV}$, a discrepancy between full RG results and leading log approximation is of about one order of magnitude at $M_{1=2} = 1 \text{ TeV}$, while for $m_0 = 300 \text{ GeV}$, this is reduced to be about a factor of two. The size of discrepancy depends weakly on the scale of right-handed Majorana neutrino masses [28].

is generated by the CP violating out-of-equilibrium decay of heavy right-handed Majorana neutrinos. Let us consider the CP asymmetry parameter ϵ_i , which is generated in the decay of i -th generation of right-handed Majorana neutrino N_i . The ϵ_i is defined as

$$\epsilon_i = \frac{(N_i \bar{N}_i H L) - (N_i \bar{N}_i \bar{H} \bar{L})}{(N_i \bar{N}_i H L) + (N_i \bar{N}_i \bar{H} \bar{L})}; \quad (4.1)$$

where H and L are the ordinary Higgs and lepton doublet. At tree level, the decay width of N_i can be easily calculated as :

$$\Gamma_i^0 = \frac{(Y Y^Y)_{ii}}{8} M_i; \quad (4.2)$$

As seen in (4.2), even if the Yukawa coupling matrix Y contains complex elements, CP symmetry is not violated at tree level. Therefore, we should consider the one-loop contributions. It is well-known that CP is violated in the interference between the tree diagram and one-loop self-energy and vertex correction diagrams. Summing up the one-loop vertex and self-energy corrections, the CP asymmetry is given by

$$\epsilon_i = \frac{v_i}{s_i} = \frac{1}{8} \frac{1}{(Y Y^Y)_{ii}} \sum_{j \neq i} \text{Im} [(Y Y^Y)_{ij}^2] [v(x) + s(x)]; \quad (4.3)$$

where $v(x)$ and $s(x)$ are the self-energy and vertex correction functions with $x = M_j^2/M_i^2$ [31]. In the minimal supersymmetric standard model (MSSM) with right-handed neutrinos, they are given by [31, 32]

$$v(x) = \frac{p}{x} \ln \frac{1+x}{x}; \quad s(x) = \frac{(M_j^2 - M_i^2) M_i M_j}{(M_j^2 - M_i^2)^2 + M_i^2 (\frac{p}{x})^2} = \frac{(x-1) \frac{p}{x}}{(x-1)^2 + (\frac{p}{x})^2} = \frac{(x-1) \frac{p}{x}}{x^2 - 2x + 1 + \frac{p^2}{x^2}}; \quad (4.4)$$

which is available for both cases of the hierarchical case and the quasi-degenerate case of M_i and M_j .

In order to calculate the baryon asymmetry, we need to solve the Boltzmann equations in thermal leptogenesis scenario [33]. We can use the approximate solution of these Boltzmann equations as

$$\epsilon_B = \frac{0.01}{\epsilon_i} \frac{x}{x_i}; \quad (4.5)$$

where ϵ_B is baryon asymmetry of the universe, ϵ_i is so-called dilution factor which describe the wash-out effect of generated lepton asymmetry. The ϵ_i is approximated as [34]

$$\epsilon_i = 0.3 \frac{10; 3 \text{eV}}{m_i} \ln \frac{m_i}{10; 3 \text{eV}}^{1/0.6}; \quad m_i = \frac{(M_D M_D^Y)_{ii}}{M_i}; \quad (4.6)$$

In the following, we compare the current range of observed baryon asymmetry [35] :

$$\epsilon_B = (6.2 - 6.9) \cdot 10^{10}; \quad (4.7)$$

with the predicted values of our model.

It is convenient to discuss the hierarchical case : $M_1 < M_2, M_3$ and degenerate case : $M_1 = M_2 = M_3$ of right-handed Majorana masses, separately. For the hierarchical case, from the model independent analyses of thermal leptogenesis [36, 37], the lightest Majorana neutrino mass must satisfy the condition :

$$M_1 > 4.9 \times 10^8 \text{ GeV} ; \quad (4.8)$$

to generate the observed baryon asymmetry of the universe. The case II, III and IV correspond to the hierarchical case. In these cases, as shown in the numerical results of tables, the lightest Majorana neutrino mass M_1 is lighter than $4.9 \times 10^8 \text{ GeV}$ for all types to satisfy the conditions of the current neutrino experiments. Therefore, it is impossible to explain the observed baryon asymmetry by thermal leptogenesis for the case of II, III and IV.

On the other hand, the case I corresponds to the degenerate case : $M_1 = M_2 = M_3$. This case satisfies the relation : $M_2 = M_1 + M_2$. It is easy to find in eqs. (4.4) that there occurs an enhancement of CP asymmetry for some region of the degeneracy and $\epsilon_i = 0$ for the case of exact degeneracy : $M_1 = M_2$. The scenario utilizing this enhancement is called as "resonant leptogenesis" [38, 39]. Some author showed that observed baryon asymmetry can be generated with considerably light right-handed neutrino masses, in complete accordance with the current solar and atmospheric neutrino experiments [39, 40, 41, 42]. This is a candidate to solve the gravitino problem [43].

The mass eigenvalues of right-handed Majorana neutrinos for the case I are exactly degenerate : $M_1 = M_2 = rM_3 = 10^9 \text{ GeV}$. However, it is natural to explain that the mass spectrum may be somewhat deviated from exact degeneracy by, for example, quantum corrections. Let us define the degree of degeneracy for M_1 and M_2 by

$$M = \frac{M_2}{M_1} = 1 : \quad (4.9)$$

The predicted baryon asymmetry is shown in Figure 17 as a function of M . As seen in Figure 17, if the degree of degeneracy is the level of $M = 10^{-3}$, the predicted asymmetry is consistent with the observed value for the type S_1 in the case I. It is concluded that the baryon asymmetry can be explained by the resonant leptogenesis scenario in the suitable region of the mass degeneracy in our model. Almost the same result is obtained for the type S_2 .

5 Summary

We have investigated the symmetric 2-zero texture of neutrino mass matrix for the possible four textures of the right-handed Majorana neutrino together with the Dirac neutrino mass matrix with two zeros, under the SUSY SO(10) GUT model including the Pati-Salam symmetry. We made a full analysis for the parameters included in such four cases of neutrino mass matrices and showed how they are consistently explain the neutrino masses and mixing angles as well as the baryon number in the Universe via leptogenesis.

In the case I, which has the simplest form of right-handed Majorana neutrino mass matrix with two parameters as seen in eq. (2.28), the class S is consistent with the current neutrino

experimental data, if we are allowed to take a little larger the value of up quark mass at the GUT scale. On the contrary, in the other three cases which are slightly extended to more general cases within 2-zero texture, having one or two new parameters as seen in eq. (2.30), (2.31) and (2.32), it is shown that the type S_1 and S_2 have the experimentally allowed regions in the case II, the types C_1 , F_3 and F_4 in the case III, and the types S_1 , S_2 , A_1 , B_1 , C_1 , F_3 and F_4 in the case IV. We found that the prediction of $|U_{e3}|$ depends on the types of Dirac neutrino and right-handed Majorana mass matrix, considerably.

We have also calculated the branching ratios of LFV processes for the type S_1 and S_2 . The predicted branching ratios are well below the experimental upper bounds except ! process for the case S_1 . On the other hand, for the case II, III and IV, the predicted branching ratios are almost same as the case I. Also, we have discussed the thermal leptogenesis in our model. Because in the case II, III and IV corresponding to the hierarchical case, the lightest Majorana neutrino mass M_1 is lighter than 4.9×10^6 GeV for all types to satisfy the conditions of the current neutrino experiments, it is impossible to explain the observed baryon asymmetry by thermal leptogenesis for the case of II, III and IV.

In summary, we have shown that only the class S in the case I, having degenerate mass spectrum for the 1st and 2nd generation of right-handed Majorana neutrino, can simultaneously explain the current neutrino experimental data, lepton flavor violating process and baryon asymmetry of the Universe. The precision measurements for neutrino mixings and mass-squared differences, furthermore, LFV will test if such model is realized in Nature in near future.

Acknowledgements

This collaboration has been encouraged by the stimulating discussion in the Summer Institutes 2003. We would like to thank to N. Okamura who encouraged us very much on the post-NOON04 informal meeting held at Ochanomizu Univ. We would also like to thank T. Yamashita for giving us useful comments on writing Appendix C. M. Bando and M. Tanimoto are supported in part by the Grant-in Aid for Scientific Research No.12047225 and 12047220.

Appendix A: Phases in neutrino mass matrices

The complex symmetric matrices are given for the Dirac and Majorana neutrinos as follows:

$$M_D = \begin{pmatrix} 0 & 0 & a & 0 & 1 \\ \bar{B} & a & b & \bar{C} & m_t \end{pmatrix}; \quad M_R = \begin{pmatrix} 0 & 0 & r & 0 & 1 \\ \bar{B} & r & 0 & \bar{C} & M_3 \\ 0 & c & d & 0 & 1 \end{pmatrix}; \quad (A.1)$$

where each element is complex in general except for M_3 and m_t . The matrix M_R is transformed to the real symmetric matrix by phase matrix P_R

$$M_R \rightarrow \overline{M}_R = P_R M_R P_R = \begin{pmatrix} 0 & 0 & \bar{r} & 0 & 1 \\ \bar{B} & \bar{r} & 0 & \bar{C} & M_3 \\ 0 & 0 & 1 \end{pmatrix}; \quad P_R = \begin{pmatrix} 0 & e^{i\phi} & 0 & 0 & 1 \\ \bar{B} & 0 & e^{i(\phi+\pi)} & \bar{C} & 0 \\ 0 & 0 & 0 & 0 & 1 \end{pmatrix}; \quad (A.2)$$

where $\theta = \arg[r]$.

On the other hand, the Dirac neutrino mass matrix turns to

$$M_D = \overline{M}_D = P_R M_D P = \begin{pmatrix} 0 & 0 & \frac{1}{2} & 0 & 0 & 0 & 0 \\ 0 & 0 & \frac{1}{2} & 0 & 0 & 0 & 0 \\ \frac{1}{2} & \frac{1}{2} & 0 & 0 & 0 & 0 & 0 \\ 0 & 0 & 0 & 0 & 0 & 0 & 0 \\ 0 & 0 & 0 & 0 & 0 & 0 & 0 \\ 0 & 0 & 0 & 0 & 0 & 0 & 0 \end{pmatrix} \quad (A.3)$$

where

$$\begin{aligned} \theta &= 2 \arg[a] + \arg[c] ; & \theta &= \arg[c] ; \\ \theta &= \arg[a] ; & \theta &= \arg[c] - \arg[a] ; \\ \theta_1 &= \arg[a] + \arg[b] - 2 \arg[c] + \dots ; & \theta_2 &= \arg[a] + \arg[d] + \dots : \end{aligned} \quad (A.4)$$

By using the seesaw formula, we have neutrino mass matrix

$$M = M_D^T M_R^{-1} M_D = P \overline{M} P \quad (A.5)$$

where

$$\begin{aligned} \overline{M} &= \overline{M}_D^T \overline{M}_R^{-1} \overline{M}_D \\ &= \begin{pmatrix} 0 & 0 & \frac{1}{2} & 0 & 0 & 0 & 0 \\ 0 & 0 & \frac{1}{2} & 0 & 0 & 0 & 0 \\ \frac{1}{2} & \frac{1}{2} & 0 & 0 & 0 & 0 & 0 \\ 0 & 0 & 0 & 0 & 0 & 0 & 0 \\ 0 & 0 & 0 & 0 & 0 & 0 & 0 \\ 0 & 0 & 0 & 0 & 0 & 0 & 0 \end{pmatrix} \frac{m_t^2}{2M_3} : \end{aligned} \quad (A.6)$$

Taking account the hierarchy of parameters $\frac{1}{2}, \frac{1}{4}, \frac{1}{4}, \frac{1}{4}, \frac{1}{4}$ and $\frac{1}{2}, \frac{1}{2}, \frac{1}{2}, \frac{1}{2}$ with $\theta = 0.2$, we get

$$\overline{M} = \begin{pmatrix} 0 & 0 & \frac{1}{2} & 0 & 0 & 0 & 0 \\ 0 & 0 & \frac{1}{2} & 0 & 0 & 0 & 0 \\ \frac{1}{2} & \frac{1}{2} & 0 & 0 & 0 & 0 & 0 \\ 0 & 0 & 0 & 0 & 0 & 0 & 0 \\ 0 & 0 & 0 & 0 & 0 & 0 & 0 \\ 0 & 0 & 0 & 0 & 0 & 0 & 0 \end{pmatrix} \frac{m_t^2}{2M_3} : \quad (A.7)$$

By using another phase matrix P^0 , \overline{M} turns to

$$M = P^0 \overline{M} P^0 = \begin{pmatrix} 0 & 0 & \frac{1}{2} & 0 & 0 & 0 & 0 \\ 0 & 0 & \frac{1}{2} & 0 & 0 & 0 & 0 \\ \frac{1}{2} & \frac{1}{2} & 0 & 0 & 0 & 0 & 0 \\ 0 & 0 & 0 & 0 & 0 & 0 & 0 \\ 0 & 0 & 0 & 0 & 0 & 0 & 0 \\ 0 & 0 & 0 & 0 & 0 & 0 & 0 \end{pmatrix} \frac{m_t^2}{2M_3} : \quad (A.8)$$

where

$$P^0 = \begin{pmatrix} 0 & e^{i\theta_2} & 0 & 0 & 1 \\ 0 & 0 & e^{i\theta_2} & 0 & 0 \\ 0 & 0 & 0 & 0 & \frac{1}{2} \\ 0 & 0 & 0 & e^{i\theta_2} & 0 \end{pmatrix} : \quad (A.9)$$

Therefore, the neutrino mass matrix is given as

$$M = P \overline{M} P ; P = P^0 P = \begin{pmatrix} 0 & e^{i(\theta_1 - \theta_2)} & 0 & 0 & 1 \\ 0 & 0 & e^{i(\theta_1 + \theta_2)} & 0 & 0 \\ 0 & 0 & 0 & e^{i(\theta_1 - \theta_2)} & 0 \\ 0 & 0 & 0 & 0 & \frac{1}{2} \end{pmatrix} : \quad (A.10)$$

Suppose the charged lepton mass matrix M_1 to be real by the phase matrix P_1 ,

$$M_1 ! \quad \overline{M}_1 = P_1 M_1 P_1 ; \quad P_1 = \begin{pmatrix} 0 & e^{i\alpha} & 0 & 0 & 1 \\ \bar{B} & 0 & e^{i\beta} & 0 & \bar{C} \\ 0 & 0 & e^{i\gamma} & 0 & \bar{A} \end{pmatrix} ; \quad (A.11)$$

where \overline{M}_1 is real matrix. Then, the MNS matrix U_{MNS} is given by

$$U_{MNS} = O_1^T Q U ; \quad Q = P P_1 ; \quad (A.12)$$

where $U_1 = P_1 O_1$ and U are unitary matrices, which diagonalize M_1 and \overline{M}_1 , respectively. In this paper, we have parametrized

$$Q = \begin{pmatrix} 0 & 1 & 0 & 0 & 1 \\ \bar{B} & 0 & e^{i\delta} & 0 & \bar{C} \\ 0 & 0 & e^{i\epsilon} & 0 & \bar{A} \end{pmatrix} ; \quad (A.13)$$

where

$$= \alpha_1 + \beta_1 e^{i\alpha_2} + \gamma_2 e^{i\alpha_1} ; \quad = \alpha_1 + \beta_1 e^{i\alpha_2} ; \quad (A.14)$$

which are given in terms of the arguments of a, b, c, d and r .

In the leptogenesis, the effective phases are α_1 and α_2 since we calculate in the basis of the real mass matrix M_R

$$\overline{M}_D \overline{M}_D^Y = P_R M_D M_D^Y P_R ; \quad (A.15)$$

which is independent of phase matrix P . The phases α_1 and α_2 are independent of the phases β_1 and γ_2 , which appear in the MNS matrix and then, in the calculations of the lepton flavor violations such as $e^+ \rightarrow e^+$.

B Phases in the charged lepton mass matrix

The complex symmetric matrix is given for the charged lepton mass matrix as follows:

$$M_1 = \begin{pmatrix} 0 & 0 & a_1 & 0 & 1 \\ \bar{B} & a_1 & b_1 & c_1 \bar{A} & m_1 \\ 0 & c_1 & d_1 & 0 & 0 \end{pmatrix} ; \quad (B.16)$$

where a_1, b_1, c_1 and d_1 are complex in general. The mass matrix turns to

$$M_1 ! \quad \overline{M}_1 = P_1 M_1 P_1 = \begin{pmatrix} 0 & 0 & \bar{a}_1 j & 0 & 1 \\ \bar{B} & \bar{a}_1 j & \bar{b}_1 j e^{i\alpha} & \bar{c}_1 j \bar{A} & m_1 \\ 0 & \bar{c}_1 j & \bar{d}_1 j & 0 & 0 \end{pmatrix} ; \quad P_1 = \begin{pmatrix} 0 & e^{i\alpha} & 0 & 0 & 1 \\ \bar{B} & 0 & e^{i\beta} & 0 & \bar{C} \\ 0 & 0 & e^{i\gamma} & 0 & \bar{A} \end{pmatrix} ; \quad (B.17)$$

where there is still one phase after removing phases by the phase matrix P_1 . Mass eigenvalues and left-handed mixings are given by solving the following matrix

$$\overline{M}_1^Y \overline{M}_1 = \begin{pmatrix} 0 & \bar{a}_1 j & \bar{a}_1 j \bar{b}_1 j e^{i\alpha} & \bar{a}_1 j \bar{d}_1 j & 1 \\ \bar{B} & \bar{a}_1 j \bar{b}_1 j e^{i\alpha} & \bar{a}_1 j + \bar{b}_1 j + \bar{c}_1 j & \bar{a}_1 j \bar{d}_1 j + \bar{b}_1 j \bar{c}_1 j e^{i\alpha} \bar{A} m_1^2 & \bar{C} \\ \bar{a}_1 j \bar{c}_1 j & \bar{a}_1 j \bar{d}_1 j + \bar{b}_1 j \bar{c}_1 j e^{i\alpha} & \bar{a}_1 j + \bar{b}_1 j & 0 & 0 \end{pmatrix} ; \quad (B.18)$$

Due to the hierarchy of parameters β_{1j}^5 , β_{1j}^2 , β_{1j}^2 and β_{1j}^1 , the effect of the phase γ_1 is minor. The eigenvalue equation is approximately given as

$$x^3 - \beta_{1j}^2 x^2 + (\beta_{1j}^2 \beta_{1j}^2 + \beta_{1j}^2 \beta_{1j}^2 - 2\beta_{1j} \beta_{1j}^2 \beta_{1j} \cos \gamma_1) x - \beta_{1j}^2 \beta_{1j}^2 \beta_{1j}^2 = 0; \quad (B.19)$$

where non-leading terms are neglected. The term including $\cos \gamma_1$ is also a non-leading term.

By the rephasing in eq. (B.18), the phases move to the 1-3 and 3-1 elements as follows:

$$\begin{matrix} 0 & \beta_{1j}^2 & \beta_{1j} \beta_{1j} & \beta_{1j} \beta_{1j} \beta_{1j}^2 & 1 \\ P_1^y M_1^y \bar{M}_1 \bar{P}_1 = \begin{pmatrix} B & \beta_{1j} \beta_{1j} & \beta_{1j}^2 + \beta_{1j}^2 + \beta_{1j}^2 & \beta_{1j} \beta_{1j} \beta_{1j}^2 + \beta_{1j} \beta_{1j} \beta_{1j}^2 & C m_1^2 \\ \beta_{1j} \beta_{1j} & \beta_{1j}^2 + \beta_{1j}^2 + \beta_{1j}^2 & \beta_{1j} \beta_{1j} \beta_{1j}^2 + \beta_{1j} \beta_{1j} \beta_{1j}^2 & \beta_{1j}^2 + \beta_{1j}^2 & \\ \beta_{1j} \beta_{1j} \beta_{1j}^2 & \beta_{1j} \beta_{1j} \beta_{1j}^2 + \beta_{1j} \beta_{1j} \beta_{1j}^2 & \beta_{1j}^2 + \beta_{1j}^2 & & \end{pmatrix} \\ & \beta_{1j} \beta_{1j} \beta_{1j}^2 & \beta_{1j} \beta_{1j} \beta_{1j}^2 + \beta_{1j} \beta_{1j} \beta_{1j}^2 & \beta_{1j}^2 + \beta_{1j}^2 & \end{matrix} \quad (B.20)$$

where $\gamma_1 = \gamma_1$ and

$$\begin{matrix} 0 & e^{i\gamma_1} & 0 & 0 & 1 \\ \bar{P}_1' = \begin{pmatrix} B & 0 & 1 & 0 & C \\ 0 & 0 & 1 & & \\ & & & & \end{pmatrix} & & & & \end{matrix} \quad (B.21)$$

after neglecting non-leading terms. Therefore, the imaginary part appears only in the (1-3) mixing, in which the absolute value is very small compared with other mixings. In conclusion, the effect of the phase γ_1 can be neglected in practice.

C The effect of deviation from m_2

The following two-zero texture

$$M = \begin{matrix} 0 & 0 & A & 0 & 1 \\ B & A & B & C & C \\ 0 & C & D & & \end{matrix} \quad (C.1)$$

has the relations between its components and mass eigenvalues as follows:

$$B + D = m_1 + m_2 + m_3; \quad (C.2)$$

$$BD - C^2 = m_1 m_2 + m_2 m_3 + m_3 m_1; \quad (C.3)$$

$$DA^2 = m_1 m_2 m_3; \quad (C.4)$$

If we take $B = m_2$ ($= B_0$) and $D = m_3 + m_1$ ($= D_0$), the remaining components can be obtained as [12]

$$A = \frac{s}{m_3 + m_1} \frac{(-m_1)m_2 m_3}{(m_3 + m_1)} (-A_0); \quad C = \frac{s}{m_3 + m_1} \frac{(-m_1)m_3 (m_3 - m_2 + m_1)}{(m_3 + m_1)} (-C_0); \quad (C.5)$$

Hereafter, we will transform m_1 into m_1 by rephasing. Without the loss of generality, we can consider a small deviation " from m_2 in the 2-2 component of M :

$$B = m_2 + " = B_0 (1 + "^0); \quad (C.6)$$

$$D = m_3 - m_1 - " = D_0 (1 - ""); \quad (C.7)$$

where $"^0 = "m_2$, $" = "m_3$. Then, we obtain

$$A = \frac{s \overline{m_1 m_2 m_3}}{D_0 (1 - ")} , \quad A_0 (1 - ")^{1=2} : \quad (C.8)$$

and

$$\begin{aligned} C^2 &= m_1 m_2 m_2 m_3 + m_3 m_1 + B D \quad A^2 \\ &= m_1 m_2 m_2 m_3 + m_3 m_1 + B_0 D_0 \quad A_0^2 + B_0 D_0 "^0 \\ &= C_0^2 + B_0 D_0 "^0 \\ &= C_0^2 + B_0 D_0 "^0 \quad 1 + \frac{B_0 D_0 "^0}{C_0^2} : \end{aligned} \quad (C.9)$$

Here, we can calculate

$$\frac{B_0 D_0 "^0}{C_0^2}, \quad \frac{m_2 "}{m_1 m_2} = \frac{"}{m_1} : \quad (C.10)$$

In the case I ($" = 0$), we needed to enlarge the range of up quark mass at the GUT scale in order for the class S to get the overlapped region on $\{\}$ plane. We, here, examine whether or not we can obtain the overlapped region by the effect of deviation from m_2 , instead of taking a wider range of up quark mass.

With eqs. (C.6), (C.7), (C.8) and (C.9), the Dirac neutrino mass matrix is given as

$$M_D = \begin{pmatrix} 0 & 0 & a_0 & 0 \\ 0 & a_0 & a_0 (1 + "^0) & c_0 (1 + \frac{b_0 d_0 "^0}{c_0^2})^{1=2} \frac{C}{A} m_t \\ 0 & c_0 (1 + \frac{b_0 d_0 "^0}{c_0^2})^{1=2} & d_0 & 0 \end{pmatrix} \quad (C.11)$$

where we take $a = a_0$ and $d = d_0$ because of $" = "^0$. Then, the neutrino mass matrix is given as

$$M = \begin{pmatrix} 0 & 0 & 0 & 1 \\ 0 & h \frac{C}{A} \frac{d^2 m_t^2}{M_3} & 0 & 0 \\ 0 & 0 & 0 & 1 \end{pmatrix}, \quad \text{with} \quad M_R = \begin{pmatrix} 0 & r & 0 & 1 \\ 0 & r & 0 & 0 \\ 0 & 0 & 0 & 1 \end{pmatrix} M_3; \quad (C.12)$$

where

$$h = \frac{ac}{rd^2}; \quad \frac{2ab}{rd^2}; \quad \frac{a^2}{rd^2}; \quad (C.13)$$

The values of a and d are determined by a parameter r , or equivalently h :

$$a = \frac{2b}{c}h; \quad d = \frac{a}{c}h; \quad (C.14)$$

from which we can finally obtain

$$a = h \frac{b_0 (1 + "^0)}{c_0 (1 + \frac{b_0 d_0 "^0}{c_0^2})^{1=2}}, \quad d = \frac{1}{2} \frac{"}{m_1}; \quad (C.15)$$

$$d = h \frac{a_0}{c_0 (1 + \frac{b_0 d_0 "^0}{c_0^2})^{1=2}}, \quad a = \frac{1}{2} \frac{"}{m_1}; \quad (C.16)$$

As we can see in eqs. (C.15) and (C.16), the change of $"$ affects both a and d equally, although we have seen that enlarging the range of up quark mass made only a decrease in the case I ($" = 0$). Therefore, we cannot arrive at the overlapped region by taking the effect of deviation from m_2 . This has been also confirmed by numerical calculation.

References

[1] G. L. Fogli, E. Lisi, M. M. Garrone, D. M. Montanino, A. Palazzo and A. M. Rotunno, *Phys. Rev. D* 67 (2003), 073002;
 J. N. Bahcall, M. C. Gonzalez-Garcia and C. Pena-Garay, *JHEP* 0302 (2003), 009;
 M. Maltoni, T. Schwetz and J.W. F. Valle, *Phys. Rev. D* 67 (2003), 093003;
 P.C. Holanda and A.Yu. Smirnov, *JCAP* 0302 (2003), 001;
 V. Barger and D. Marfatia, *Phys. Lett. B* 555 (2003), 144;
 M. Maltoni, T. Schwetz, M. Tortola and J.W. F. Valle, [hep-ph/0309130](#).

[2] Super-Kamiokande Collaboration, Y. Fukuda et al., *Phys. Rev. Lett.* 81, 1562 (1998);
ibid. 82, 2644 (1999); *ibid.* 82, 5194 (1999);
 K. Nishikawa, Invited talk at XXI Lepton Photon Symposium, August 10–16, 2003, Batavia, USA.

[3] Super-Kamiokande Collaboration, S. Fukuda et al., *Phys. Rev. Lett.* 86, 5651; 5656 (2001).

[4] SNO Collaboration: Q. R. Ahmad et al., *Phys. Rev. Lett.* 87, 071301 (2001), *ibid.* 89, 011301 (2002), *ibid.* 89, 011302 (2002), [nucl-ex/309004](#).

[5] KamLAND Collaboration, K. Eguchi et al., *Phys. Rev. Lett.* 90, 021802 (2003).

[6] CHOOZ Collaboration, M. Apollonio et al., *Phys. Lett. B* 466, 415 (1999).

[7] H. Georgi and C. Jarlskog, *Phys. Lett. B* 86 (1979), 297.

[8] M. Bando, S. Kaneko, M. Obara and M. Tanimoto, *Phys. Lett. B* 580 (2004), 229.

[9] Z. Maki, M. Nakagawa and S. Sakata, *Prog. Theor. Phys.* 28 (1962), 870.

[10] See the Nishiura, Matsuura and Fukuyama in reference [12] for the matrix form of O_1 .

[11] N. Haba, Y. Matsuura, N. Okamura and M. Sugiura, *Eur. Phys. J. C* 10 (1999) 677; *Prog. Theor. Phys.* 103 (2000), 145;
 N. Haba and N. Okamura, *Eur. Phys. J. C* 14 (2000) 347;
 N. Haba, N. Okamura and M. Sugiura, *Prog. Theor. Phys.* 103 (2000), 367.

[12] H. Nishiura, K. Matsuura and T. Fukuyama, *Phys. Rev. D* 60 (1999), 013006;
 K. Matsuura, T. Fukuyama and H. Nishiura, *Phys. Rev. D* 61 (2000), 053001.

[13] J. Harvey, P. Ramond and D. Reiss, *Phys. Lett. B* 92 (1980), 309; *Nucl. Phys. B* 199 (1982), 223.

[14] Y. Achiman and T. G. Reiner, *Nucl. Phys. B* 443 (1995), 3.

[15] S. Dimopoulos, L. J. Hall and S. Raby, *Phys. Rev. Lett.* 68 (1992), 1984; *Phys. Rev. D* 45 (1992), 4195.

[16] M. Bando and M. Obara, *Prog. Theor. Phys.* 109 (2003), 995.

[17] H .Fritzsch and Z-Z.X ing, *Prog. Part. Nucl. Phys.* 45 (2000), 1.

[18] F .Borzum ati and A .M asiero, *Phys. Rev. Lett.* 57 (1986) 961.

[19] J.H isano, T .M oroi, K .Tobe, M .Yam aguchi and T .Yanagida, *Phys. Lett.B* 357 (1995) 579;
J. H isano, T .M oroi, K .Tobe and M .Yam aguchi, *Phys. Rev. D* 53 (1996) 2442.

[20] J. H isano, D .N omura and T .Yanagida, *Phys. Lett. B* 437 (1998) 351;
J. H isano and D .N omura, *Phys. Rev. D* 59 (1999) 116005;
M .E .G om ez, G K .Leontaris, S .Lola and J. D .V ergados, *Phys. Rev. D* 59 (1999) 116009;
W .Budm uller, D .D elapine and F .V issani, *Phys. Lett. B* 459 (1999) 171;
W .Budm uller, D .D elapine and L.T .H andoko, *Nucl. Phys. B* 576 (2000) 445;
J. E llis, M .E .G om ez, G K .Leontaris, S .Lola and D .V .N anopoulos, *Eur. Phys. J. C* 14 (2000) 319;
J. L .F eng, Y .N ir and Y .Shadm i, *Phys. Rev. D* 61 (2000) 113005;
S .Baek, T .G oto, Y .O kada and K .O kumura, *Phys. Rev. D* 63 (2001) 051701.

[21] J. Sato, K .Tobe, and T .Yanagida, *Phys. Lett. B* 498 (2001) 189;
J. Sato and K .Tobe, *Phys. Rev. D* 63 (2001) 116010;
S .Lavignac, I. M asina and C .A .Savoy, *Phys. Lett. B* 520 (2001) 269;
J. A .Casas and A .I barra, *Nucl. Phys. B* 618 (2001) 171;
A .K ageyama, S .K aneko, N .S im oyama and M .T animoto, *Phys. Lett. B* 527 (2002) 206; *Phys. Rev. D* 65 (2002) 096010.

[22] J. A .Casas and A .I barra, *Nucl. Phys. B* 618 (2001) 171.

[23] A .K ageyama, S .K aneko, N .S im oyama and M .T animoto, *Phys. Lett. B* 527 206 (2002);
Phys. Rev. D 65 096010 (2002).

[24] J. E llis, J. H isano, M .R aidal and Y .Shim izu, *Phys. Rev. D* 66 115013 (2002).

[25] M EGA Collaboration, M .L .B rooks et al., *Phys. Rev. Lett.* 83 (1999) 1521.

[26] K .Inam i, for the B elle collaboration, Talk presented at the 19th InternationalW orkshop on W eak Interactions and N eutrinos (W IN -03), October 6th to 11th, 2003, Lake G eneva, W isconsin, U SA .

[27] K Abe et al. (B elle collaboration), [hep-ex/0310029](#).

[28] S.T .Petcov, S .P rofum o, Y .Takanishi and C E .Yaguna, *Nucl. Phys. B* 676 (2004) 453.

[29] K .Inam i, T .H okue and T .O hshima, *eConfC* 0209101 (2002) TU11 [[hep-ex/0210036](#)].

[30] M .Fukugita and T .Yanagida, *Phys. Lett. B* 175 (1986) 45.

[31] M .F lanz, E .A .Paschos and U .Sarkar, *Phys. Lett. B* 345 (1995) 248;
L .C ovi, E .R oulet and F .V issani, *Phys. Lett. B* 384 (1996) 169;
A .P ilaftsis, *Phys. Rev. D* 56 (1997) 5431.

[32] W .Buchm uller and M .P lum acher, *Phys. Lett. B* 389 (1996) 73; *ibid. B* 431 (1998) 354; *Int. J. Mod. Phys. A* 15 (2000) 5047.

[33] M .Luty, *Phys. Rev. D* 45 (1992) 455;
M .P lum acher, *Z. Phys. C* 74 (1997) 549;
E.W .K olb and M .S.Turner, *The early universe*, Redwood City, USA :Addison-W esley (1990), (Frontiers in physics, 69);
M .Flanz and E .A .Paschos, *Phys. Rev. D* 58 (1998) 113009;

[34] H B .Nielsen and Y .Takanishi, *Phys. Lett.* 507 241 (2001).

[35] D N .Spergel et al., *Astrophys. J. Suppl.* 148, 175 (2003).

[36] W .Buchm uller, P .Di Bari and M .P lum acher, *Nucl. Phys. B* 643 (2002) 367; *Phys. Lett. B* 547 (2002) 128.

[37] G F .Giudice, A .Notari, M .Raidal, A .Riotto and A .Strumia, *Nucl. Phys. B* 685 (2004) 89.

[38] A .Pilaftsis, *Phys. Rev. D* 56 (1997) 5431; *Int. J. Mod. Phys. A* 14 (1999) 1811.

[39] A .Pilaftsis and Thomas E J.Underwood, [hep-ph/0309342](#).

[40] J.Ellis, M .Raidal and T .Yanagida, *Phys. Lett. B* 546 228 (2002).

[41] E .K .Akhmedov, M .Frigerio and A .Yu .Smirnov, *JHEP* 0309 021 (2003).

[42] C .H .A bright and S M .Barr, [hep-ph/0404095](#).

[43] M .Y .Khlopov and A .D .Linde, *Phys. Lett. B* 138 (1984) 265;
J.Ellis, J.E .K im and D .V .Nanopoulos, *Phys. Lett. B* 145 (1984) 181;
M .Kawasaki and T .Moroi, *Prog. Theor. Phys.* 93 (1995) 879.
M .Kawasaki, K .Kohri and T .Moroi, *Phys. Rev. D* 63 (2001) 103502 ; [astro-ph/0402490](#).

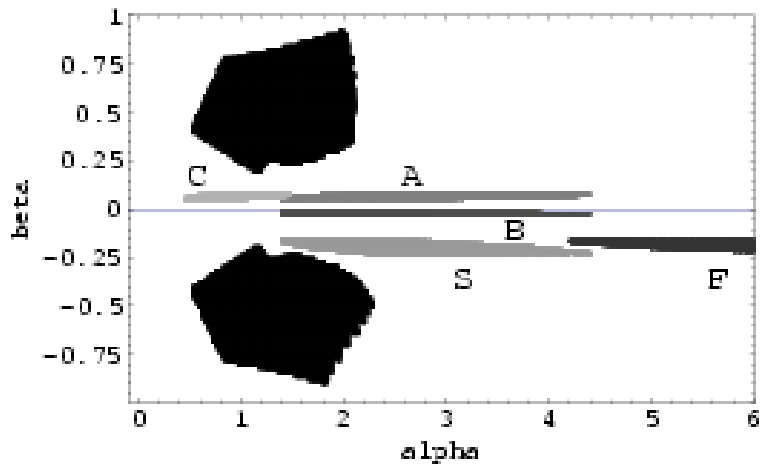


Figure 1: The black region is the experimentally allowed region predicted from a neutrino mass matrix with two zeros of eq. (2.1). The region predicted from the up-quark masses at the GUT scale for five classes S, A, B, C and F in the case I with $h = 1:3$.

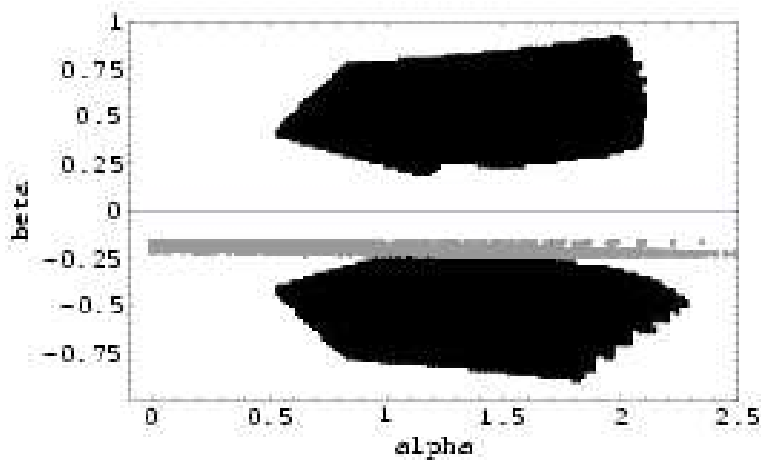


Figure 2: The black region is the experimentally allowed region predicted from a neutrino mass matrix with two zeros of eq. (2.1). The gray region is predicted from the up-quark masses at the GUT scale for the type S₁ in the case II with $h = 1:3$.

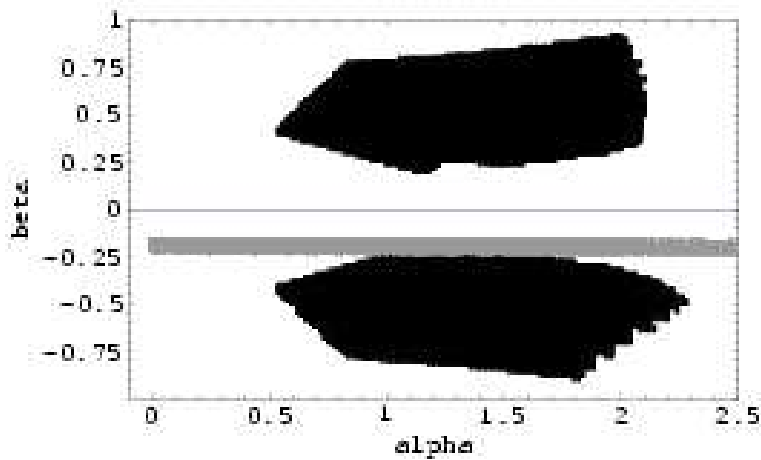


Figure 3: The black region is the experimentally allowed region predicted from a neutrino mass matrix with two zeros of eq. (2.1). The gray region is predicted from the up-quark masses at the GUT scale for the type S_2 in the case II with $h = 1:3$.

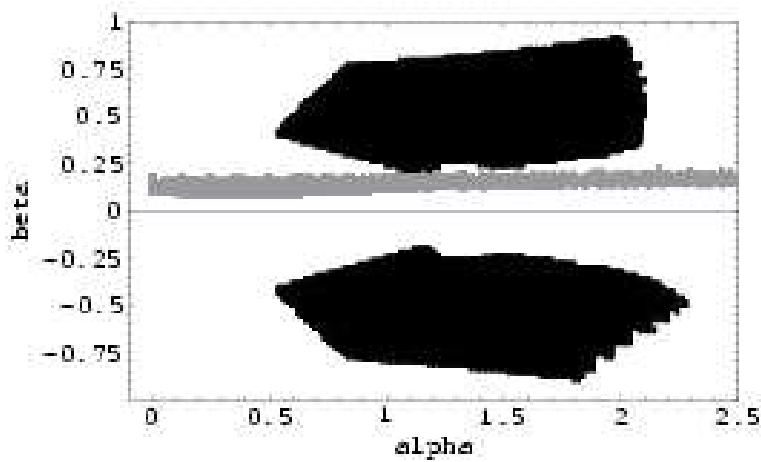


Figure 4: The black region is the experimentally allowed region predicted from a neutrino mass matrix with two zeros of eq. (2.1). The gray region is predicted from the up-quark masses at the GUT scale for the type C_1 in the case III with $h = 1:3$.

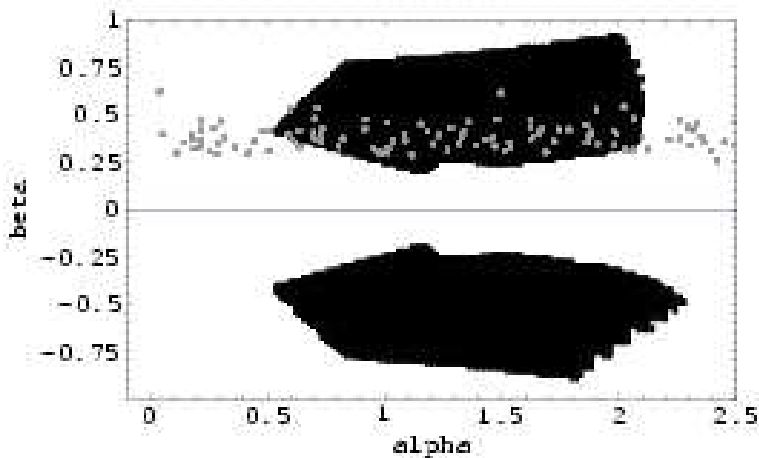


Figure 5: The black region is the experimentally allowed region predicted from a neutrino mass matrix with two zeros of eq. (2.1). The gray region is predicted from the up-quark masses at the GUT scale for the type F_3 in the case III with $h = 1:3$.

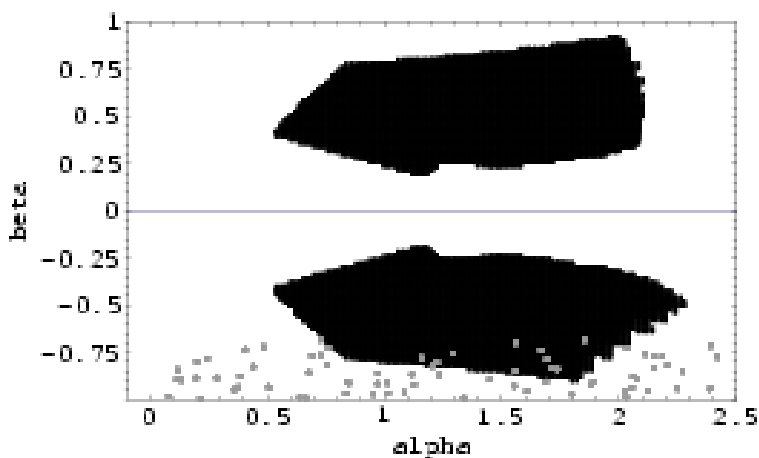


Figure 6: The black region is the experimentally allowed region predicted from a neutrino mass matrix with two zeros of eq. (2.1). The gray region is predicted from the up-quark masses at the GUT scale for the type F_4 in the case III with $h = 1:3$.

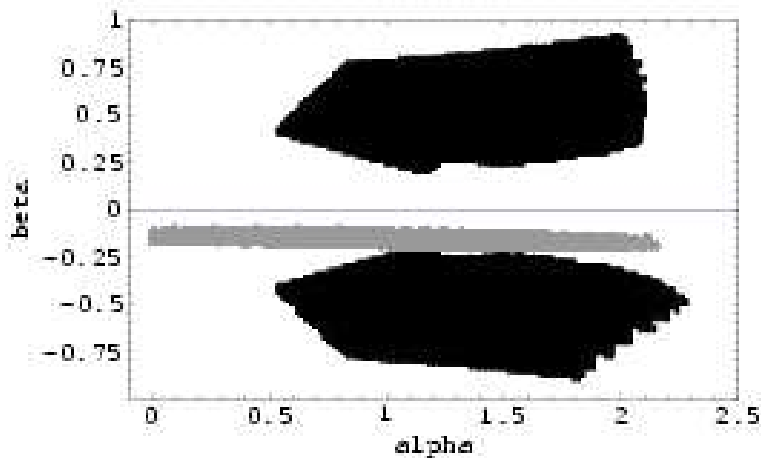


Figure 7: The black region is the experimentally allowed region predicted from a neutrino mass matrix with two zeros of eq. (2.1). The gray region is predicted from the up-quark masses at the GUT scale for the type S_1 in the case IV with $h = 1:3$.

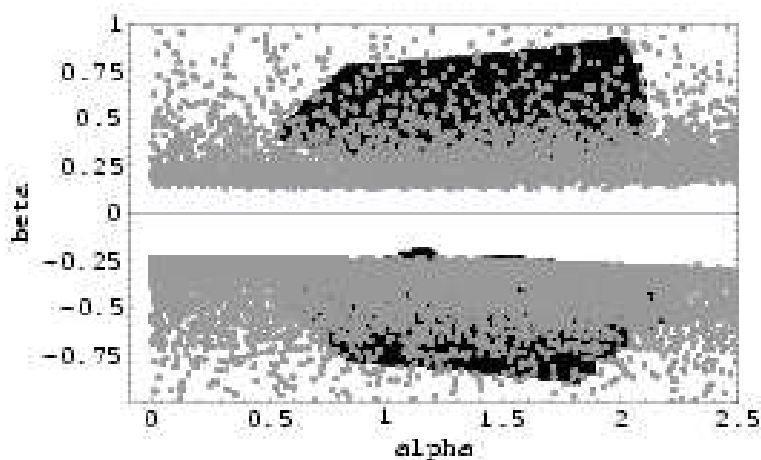


Figure 8: The black region is the experimentally allowed region predicted from a neutrino mass matrix with two zeros of eq. (2.1). The gray region is predicted from the up-quark masses at the GUT scale for the type S_2 in the case IV with $h = 1:3$.

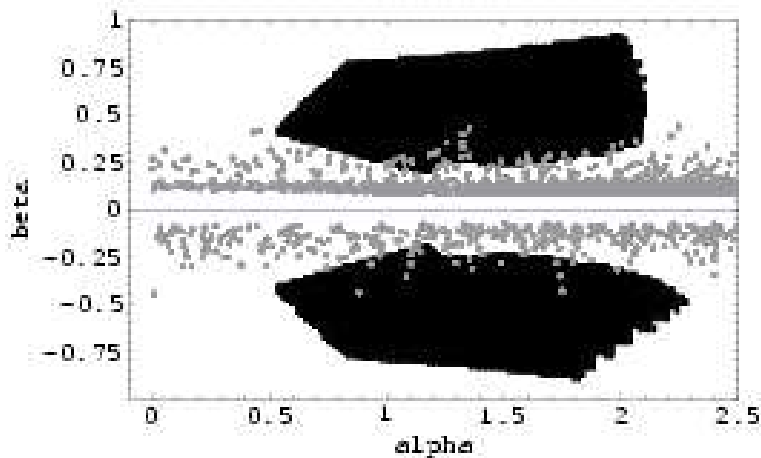


Figure 9: The black region is the experimentally allowed region predicted from a neutrino mass matrix with two zeros of eq. (2.1). The gray region is predicted from the up-quark masses at the GUT scale for the type A_1 in the case IV with $h = 1:3$.

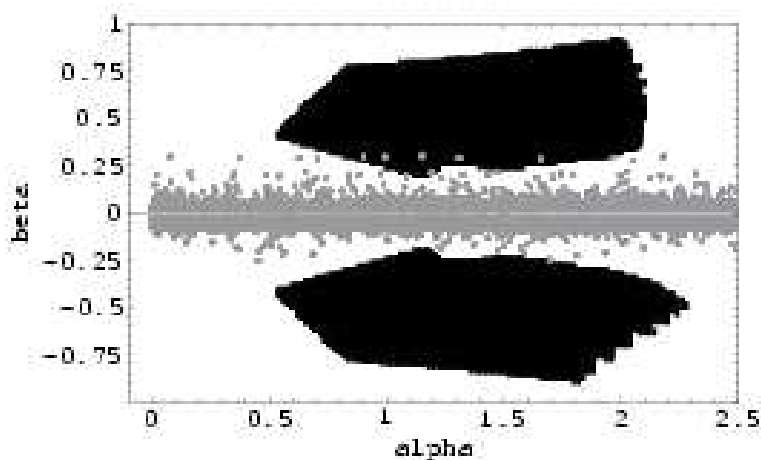


Figure 10: The black region is the experimentally allowed region predicted from a neutrino mass matrix with two zeros of eq. (2.1). The gray region is predicted from the up-quark masses at the GUT scale for the type B_1 in the case IV with $h = 1:3$.

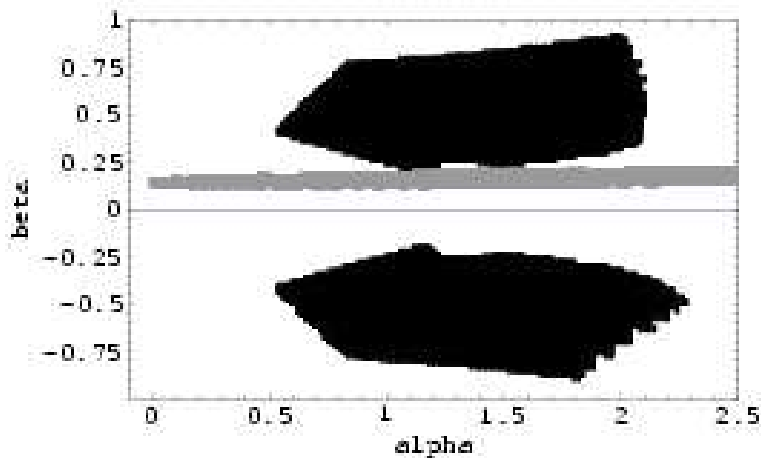


Figure 11: The black region is the experimentally allowed region predicted from a neutrino mass matrix with two zeros of eq. (2.1). The gray region is predicted from the up-quark masses at the GUT scale for the type C_1 in the case IV with $h = 1:3$.

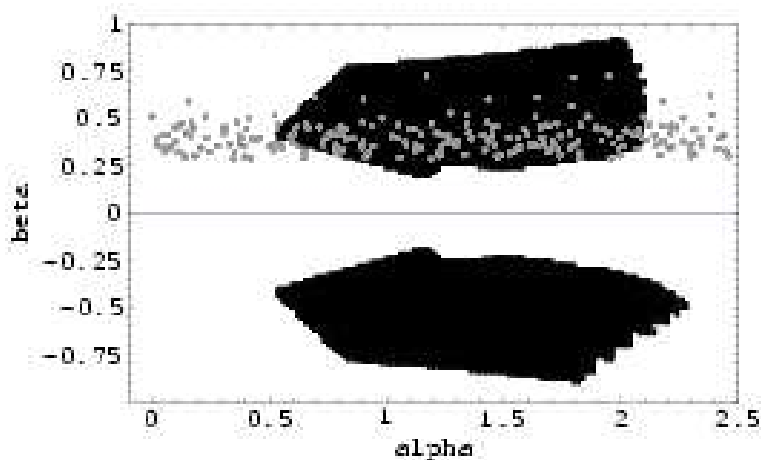


Figure 12: The black region is the experimentally allowed region predicted from a neutrino mass matrix with two zeros of eq. (2.1). The gray region is predicted from the up-quark masses at the GUT scale for the type F_3 in the case IV with $h = 1:3$.

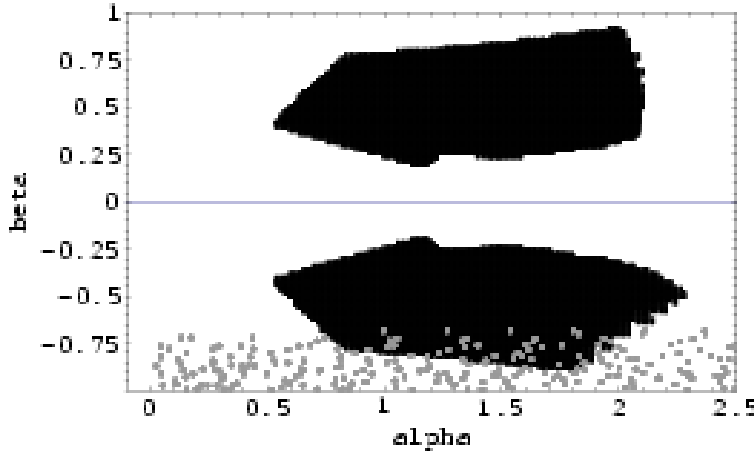


Figure 13: The black region is the experimentally allowed region predicted from a neutrino mass matrix with two zeros of eq. (2.1). The gray region is predicted from the up-quark masses at the GUT scale for the type F_4 in the case IV with $h = 1:3$.

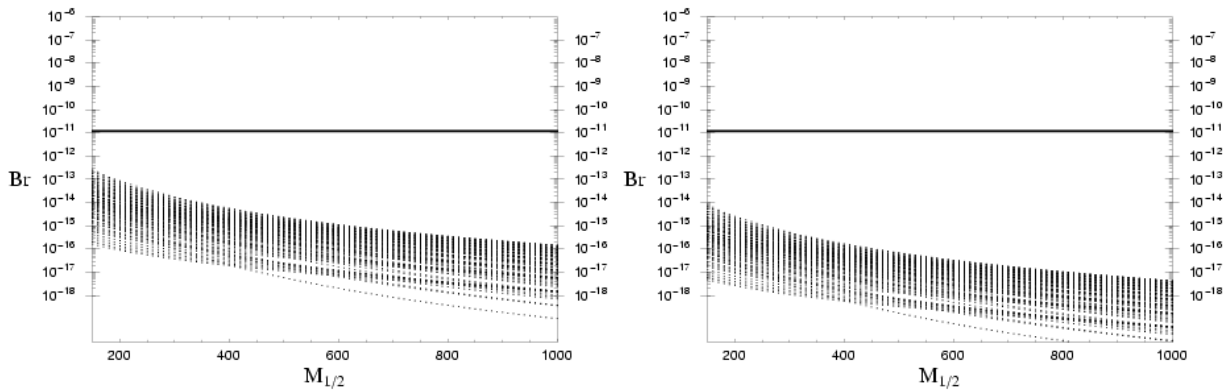


Figure 14: The predicted branching ratio of $\bar{\nu} e \rightarrow e^- \bar{\nu}$ process as a function of $M_{1/2}$ (GeV) taking $a_0 = 0, m_0 = 100$ –1000 GeV for $\tan \theta = 5$ –50 are shown. The left and right figure correspond to the type S_1 and S_2 , respectively. The horizontal line is experimental upper bound.

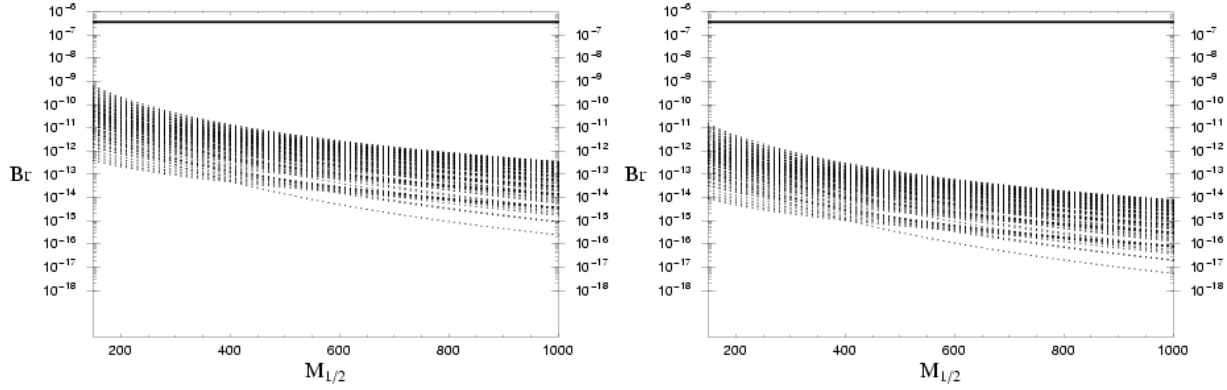


Figure 15: The predicted branching ratio of $\mu \rightarrow e$ process as a function of $M_{1/2}$ (GeV) taking $a_0 = 0, m_0 = 100 - 1000$ GeV for $\tan \theta = 5 - 50$ are shown. The left and right figure correspond to the type S_1 and S_2 , respectively. The horizontal line is experimental upper bound.

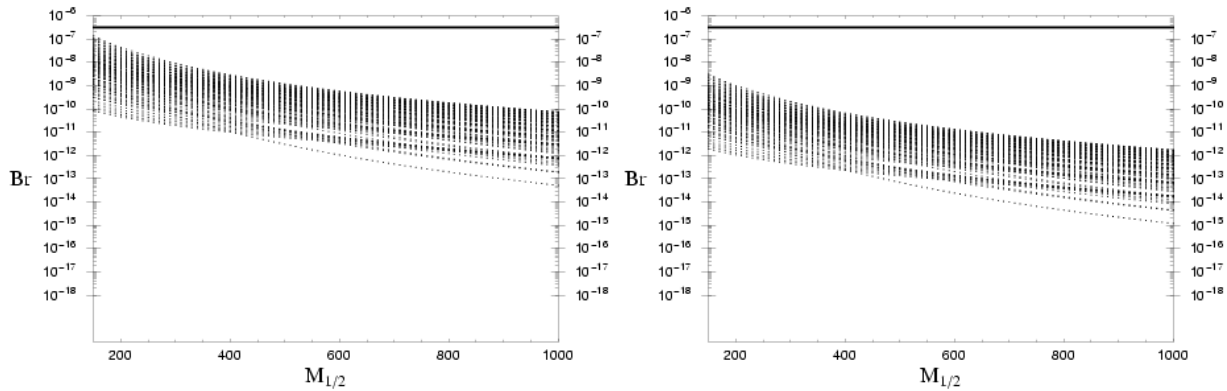


Figure 16: The predicted branching ratio of $\mu \rightarrow e$ process as a function of $M_{1/2}$ (GeV) taking $a_0 = 0, m_0 = 100 - 1000$ GeV for $\tan \theta = 5 - 50$ are shown. The left and right figure correspond to the type S_1 and S_2 , respectively. The horizontal line is experimental upper bound.

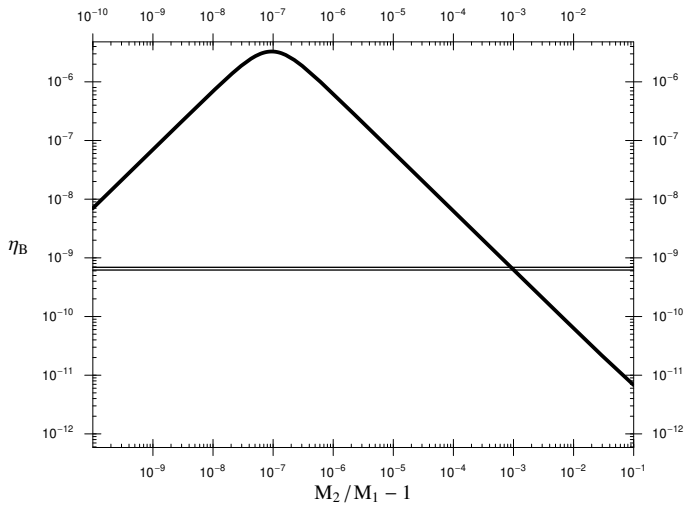


Figure 17: The predicted baryon asymmetry of the universe are shown as a function of the degeneracy M . The region between horizontal lines is the observed value of baryon asymmetry η_B [35]. The prediction is consistent with the observed value in the region of $M \gtrsim 10^{-3}$.